Obtained cells were incubated with PE anti-CD11c ($2\,\mu g\,ml^{-1}$) and subjected to cell sorting (FACSAria). $CD11c^+$ cells with >95% purity were used for the experiments. Naive B cells were purified from the spleen by negative selection using anti-CD43 microbeads (Miltenyi Biotec). Purified naive B cells (5×10^5) were cultured in the presence of $10\,\mu g\,ml^{-1}$ anti-mouse IgM $F(ab')_2$ (Jackson ImmunoResearch) alone or with equivalent numbers of Peyer's patch-derived or caecal patch-derived DCs for 4 days[32].

Whole-mount microscopic analysis. Whole-mount microscopic analysis was performed as described previously[52]. Briefly, the small and large intestines were removed intact, opened along the mesenteric border, flushed with PBS and mounted in 8-cm segments from proximal to distal. Samples were then incubated in Hank's balanced salt solution containing 5 mM EDTA at 37 °C with shaking for 10 min to remove epithelial cells, followed by washing with cold PBS. Samples were fixed in 4% paraformaldehyde for 1 h, washed with PBS-T and incubated with 1% H_2O_2 in methanol to block endogenous peroxidases. Samples were then incubated with PBS-T containing 3% BSA for 30 min with shaking, and incubated with anti-CD45R/B220 mAb ($5\,\mu g\,ml^{-1}$) overnight at 4 °C, followed by HRP-conjugated $F(ab')_2$ goat anti-rat IgG Ab (Jackson ImmunoResearch) ($1\,\mu g\,ml^{-1}$) at room temperature for 1 h. Signals were developed with Metal Enhanced DAB substrate (Thermo Scientific). Samples were analysed using an Olympus stereo microscope SZX-12.

Statistical analysis. Differences between control and experimental groups were evaluated using the Student's *t*-test. A P value <0.05 was considered statistically significant. Data are presented as mean ± s.d. Mann–Whitney *U*/Wilcoxon rank sum tests were conducted to assess significant differences in relative abundance of specific OTU obtained by microbiota analysis. For multivariate analyses of data, principal component analysis was used to visualize data sets by statistical programming language R 2.1.5. Between-class analysis and principal coordinate analysis were calculated using the R package 'ade4'. In the UniFrac analysis, ANOSIM was calculated using R package 'vegan'.

References

1. Cerutti, A. & Rescigno, M. The biology of intestinal immunoglobulin A responses. *Immunity* **28,** 740–750 (2008).
2. Pabst, O. New concepts in the generation and functions of IgA. *Nat. Rev. Immunol.* **12,** 821–832 (2012).
3. Macpherson, A. J., Geuking, M. B. & McCoy, K. D. Homeland security: IgA immunity at the frontiers of the body. *Trends Immunol.* **33,** 160–167 (2012).
4. Macpherson, A. J., Geuking, M. B., Slack, E., Hapfelmeier, S. & McCoy, K. D. The habitat, double life, citizenship, and forgetfulness of IgA. *Immunol. Rev.* **245,** 132–146 (2012).
5. Strugnell, R. A. & Wijburg, O. L. The role of secretory antibodies in infection immunity. *Nat. Rev. Microbiol.* **8,** 656–667 (2010).
6. Latiff, A. H. & Kerr, M. A. The clinical significance of immunoglobulin A deficiency. *Ann. Clin. Biochem.* **44,** 131–139 (2007).
7. Fagarasan, S. *et al.* Critical roles of activation-induced cytidine deaminase in the homeostasis of gut flora. *Science* **298,** 1424–1427 (2002).
8. Suzuki, K. *et al.* Aberrant expansion of segmented filamentous bacteria in IgA-deficient gut. *Proc. Natl Acad. Sci. USA* **101,** 1981–1986 (2004).
9. Peterson, D. A., McNulty, N. P., Guruge, J. L. & Gordon, J. I. IgA response to symbiotic bacteria as a mediator of gut homeostasis. *Cell Host Microbe* **2,** 328–339 (2007).
10. Maruya, M., Kawamoto, S., Kato, L. M. & Fagarasan, S. Impaired selection of IgA and intestinal dysbiosis associated with PD-1-deficiency. *Gut Microbe* **4,** 165–171 (2013).
11. Kawamoto, S. *et al.* The inhibitory receptor PD-1 regulates IgA selection and bacterial composition in the gut. *Science* **336,** 485–489 (2012).
12. Fritz, J. H. *et al.* Acquisition of a multifunctional IgA+ plasma cell phenotype in the gut. *Nature* **481,** 199–203 (2012).
13. Sutherland, D. B. & Fagarasan, S. IgA synthesis: a form of functional immune adaptation extending beyond gut. *Curr. Opin. Immunol.* **24,** 261–268 (2012).
14. Suzuki, K., Kawamoto, S., Maruya, M. & Fagarasan, S. GALT: organization and dynamics leading to IgA synthesis. *Adv. Immunol.* **107,** 153–185 (2010).
15. Lindner, C. *et al.* Age, microbiota, and T cells shape diverse individual IgA repertoires in the intestine. *J. Exp. Med.* **209,** 365–377 (2012).
16. Pabst, O. *et al.* Chemokine receptor CCR9 contributes to the localization of plasma cells to the small intestine. *J. Exp. Med.* **199,** 411–416 (2004).
17. Hu, S., Yang, K., Yang, J., Li, M. & Xiong, N. Critical roles of chemokine receptor CCR10 in regulating memory IgA responses in intestines. *Proc. Natl Acad. Sci. USA* **108,** E1035–E1044 (2011).
18. Mizoguchi, A., Mizoguchi, E., Chiba, C. & Bhan, A. K. Role of appendix in the development of inflammatory bowel disease in TCR-alpha mutant mice. *J. Exp. Med.* **184,** 707–715 (1996).
19. Weinstein, P. D., Anderson, A. O. & Mage, R. G. Rabbit IgH sequences in appendix germinal centers: VH diversification by gene conversion-like and hypermutation mechanisms. *Immunity* **1,** 647–659 (1994).
20. Dasso, J. F. & Howell, M. D. Neonatal appendectomy impairs mucosal immunity in rabbits. *Cell Immunol.* **182,** 29–37 (1997).
21. Clark, M. A., Jepson, M. A., Simmons, N. L. & Hirst, B. H. Differential surface characteristics of M cells from mouse intestinal Peyer's and caecal patches. *Histochem. J.* **26,** 271–280 (1994).
22. Krieglstein, C. F. *et al.* Role of appendix and spleen in experimental colitis. *J. Surg. Res.* **101,** 166–175 (2001).
23. Pollard, M. & Sharon, N. Responses of the Peyer's Patches in germ-free mice to antigenic stimulation. *Infect. Immun.* **2,** 96–100 (1970).
24. Sun, Z. *et al.* Requirement for RORgamma in thymocyte survival and lymphoid organ development. *Science* **288,** 2369–2373 (2000).
25. Shinkura, R. *et al.* Alymphoplasia is caused by a point mutation in the mouse gene encoding Nf-kappa b-inducing kinase. *Nat. Genet.* **22,** 74–77 (1999).
26. Tsuji, M. *et al.* Requirement for lymphoid tissue-inducer cells in isolated follicle formation and T cell-independent immunoglobulin A generation in the gut. *Immunity* **29,** 261–271 (2008).
27. Tezuka, H. *et al.* Prominent role for plasmacytoid dendritic cells in mucosal T cell-independent IgA induction. *Immunity* **34,** 247–257 (2011).
28. Macpherson, A. J. *et al.* A primitive T cell-independent mechanism of intestinal mucosal IgA responses to commensal bacteria. *Science* **288,** 2222–2226 (2000).
29. Tomura, M. *et al.* Monitoring cellular movement *in vivo* with photoconvertible fluorescence protein 'Kaede' transgenic mice. *Proc. Natl Acad. Sci. USA* **105,** 10871–10876 (2008).
30. Mora, J. R. & von Andrian, U. H. Differentiation and homing of IgA-secreting cells. *Mucosal Immunol.* **1,** 96–109 (2008).
31. Macpherson, A. J. & Uhr, T. Induction of protective IgA by intestinal dendritic cells carrying commensal bacteria. *Science* **303,** 1662–1665 (2004).
32. Mora, J. R. *et al.* Generation of gut-homing IgA-secreting B cells by intestinal dendritic cells. *Science* **314,** 1157–1160 (2006).
33. Eckburg, P. B. *et al.* Diversity of the human intestinal microbial flora. *Science* **308,** 1635–1638 (2005).
34. Hieshima, K. *et al.* CC chemokine ligands 25 and 28 play essential roles in intestinal extravasation of IgA antibody-secreting cells. *J. Immunol.* **173,** 3668–3675 (2004).
35. Kunkel, E. J. *et al.* CCR10 expression is a common feature of circulating and mucosal epithelial tissue IgA Ab-secreting cells. *J. Clin. Invest.* **111,** 1001–1010 (2003).
36. Rescigno, M. Intestinal dendritic cells. *Adv. Immunol.* **107,** 109–138 (2010).
37. Niess, J. H. *et al.* CX3CR1-mediated dendritic cell access to the intestinal lumen and bacterial clearance. *Science* **307,** 254–258 (2005).
38. Farache, J. *et al.* Luminal bacteria recruit CD103+ dendritic cells into the intestinal epithelium to sample bacterial antigens for presentation. *Immunity* **38,** 581–595 (2013).
39. McDole, J. R. *et al.* Goblet cells deliver luminal antigen to CD103+ dendritic cells in the small intestine. *Nature* **483,** 345–349 (2012).
40. Itohara, S. *et al.* T cell receptor delta gene mutant mice: independent generation of alpha beta T cells and programmed rearrangements of gamma delta TCR genes. *Cell* **72,** 337–348 (1993).
41. Mombaerts, P. *et al.* Mutations in T-cell antigen receptor genes alpha and beta block thymocyte development at different stages. *Nature* **360,** 225–231 (1992).
42. Eberl, G. & Littman, D. R. Thymic origin of intestinal alphabeta T cells revealed by fate mapping of RORgammat+ cells. *Science* **305,** 248–251 (2004).
43. Atarashi, K. *et al.* ATP drives lamina propria T(H)17 cell differentiation. *Nature* **455,** 808–812 (2008).
44. Andersson, A. F. *et al.* Comparative analysis of human gut microbiota by barcoded pyrosequencing. *PLoS ONE* **3,** e2836 (2008).
45. Caporaso, J. G. *et al.* QIIME allows analysis of high-throughput community sequencing data. *Nat. Methods* **7,** 335–336 (2010).
46. Quince, C., Lanzen, A., Davenport, R. J. & Turnbaugh, P. J. Removing noise from pyrosequenced amplicons. *BMC Bioinformatics* **12,** 38 (2011).
47. Edgar, R. C. Search and clustering orders of magnitude faster than BLAST. *Bioinformatics* **26,** 2460–2461 (2010).
48. Quast, C. *et al.* The SILVA ribosomal RNA gene database project: improved data processing and web-based tools. *Nucleic Acids Res.* **41,** D590–D596 (2013).
49. Cole, J. R. *et al.* The ribosomal database project (RDP-II): introducing myRDP space and quality controlled public data. *Nucleic Acids Res.* **35,** D169–D172 (2007).
50. Lozupone, C. & Knight, R. UniFrac: a new phylogenetic method for comparing microbial communities. *Appl. Environ. Microbiol.* **71,** 8228–8235 (2005).
51. Mora, J. R. *et al.* Selective imprinting of gut-homing T cells by Peyer's patch dendritic cells. *Nature* **424,** 88–93 (2003).
52. Lorenz, R. G., Chaplin, D. D., McDonald, K. G., McDonough, J. S. & Newberry, R. D. Isolated lymphoid follicle formation is inducible and dependent upon lymphotoxin-sufficient B lymphocytes, lymphotoxin beta receptor, and TNF receptor I function. *J. Immunol.* **170,** 5475–5482 (2003).

Acknowledgements

We thank M. Tomura for providing us with Kaede-transgenic mice, M. Maruya for the analysis of IgA-secreting cells, T. Kondo and Y. Magota for the maintenance of the germ-free mice and C. Hidaka for secretarial assistance. This work was supported by grants from the Ministry of Education, Culture, Sports, Science and Technology, the Japan Science and Technology Agency, and by the Ministry of Health, Labour and Welfare and The Osaka Foundation for Promotion of Clinical Immunology.

Author contributions

K.M. performed experiments. E.U., H.K., S.S., M.K., T.K., R.O. and A.T. performed animal experiments. Y.S. and M.T. performed experiments using germ-free mice. M.K., J.K., Y.B., T.K. and M.I. performed the migration experiment. S.N., D.M., T.K., K.G. and T.I. performed the pyrosequencing experiment. T.H. and O.Y. conducted the Fc-chimera protein experiment. M.F., H.K. and S.F. contributed to the experimental design and data analysis. K.T. planed and directed the research and wrote the paper.

Additional information

Supplementary Information accompanies this paper at http://www.nature.com/naturecommunications

Competing financial interests: The authors declare no competing financial interests.

Reprints and permission information is available online at http://npg.nature.com/reprintsandpermissions/

How to cite this article: Masahata, K. *et al.* Generation of colonic IgA-secreting cells in the caecal patch. *Nat. Commun.* 5:3704 doi: 10.1038/ncomms4704 (2014).

Polysaccharide A of *Bacteroides fragilis*: Actions on Dendritic Cells and T Cells

Hisako Kayama[1,2] **and Kiyoshi Takeda**[1,2,*]
[1]Laboratory of Immune Regulation, Department of Microbiology and Immunology, Graduate School of Medicine, WPI Immunology Frontier Research Center, Osaka University, Suita, Osaka 565-0871, Japan
[2]Core Research for Evolutional Science and Technology, Japan Science and Technology Agency, Saitama 332-0012, Japan
*Correspondence: ktakeda@ongene.med.osaka-u.ac.jp
http://dx.doi.org/10.1016/j.molcel.2014.04.002

In a recent paper published in *Cell Host & Microbe*, Dasgupta et al. (2014) demonstrate that a component of the gut microbiota, *Bacteroides fragilis*, induces IL-10-producing regulatory T cells by driving TLR2-dependent plasmacytoid dendritic cell activation.

Commensal microbiota in the intestine regulate the gut immune system (Hooper et al., 2012). Accordingly, dysregulation of the microbiota (known as dysbiosis) has been shown to be involved in the pathogenesis of several diseases that affect both intestinal and extraintestinal tissues. In particular, several commensal bacteria have been identified that induce the development of adaptive immunity, including IgA-secreting cells, Th1 cells, Th17 cells, and regulatory T (Treg) cells. Among these commensals, some bacteria, such as *Clostridium* species and *Bacteroides fragilis*, have been shown to modulate the immune system by inducing Treg cells (Atarashi et al., 2013; Mazmanian et al., 2008). The mechanisms of *B. fragilis*-mediated immune modulation have been intensively investigated. Capsular polysaccharide A (PSA) of *B. fragilis* induces Treg cells that secrete the potent anti-inflammatory cytokine IL-10 and thereby prevent inflammation in the gut (Mazmanian et al., 2008). A subsequent study demonstrated that PSA could directly act on TLR2 expressed by Foxp3$^+$ Treg cells to induce immune regulatory functions (Round et al., 2011). However, it is the innate immune system that generally recognizes microbes and instructs the development of T cell-mediated adaptive immune responses. Therefore, the possibility existed that PSA interactions with T cells were not the sole mechanism of PSA-mediated immune regulation.

In a recent paper published in *Cell Host & Microbe*, Dasgupta et al. (2014) analyzed the involvement of dendritic cells (DCs) in PSA-dependent modulation of the immune system. They show that plasmacytoid DCs (pDCs), but not conventional DCs (cDCs), mediate the PSA-dependent induction of IL-10-producing Treg cells. The transfer of PSA-treated pDCs ameliorates intestinal inflammation induced by trinitrobenzenesulfonic acid (TNBS). PSA-mediated IL-10 induction in Treg cells was impaired when the authors used pDCs derived from *Tlr2*$^{-/-}$ mice. The suppression of intestinal inflammation by PSA-treated pDCs requires expression of ICOSL, CD86, and MHC class II by pDCs to promote cognate interactions between pDCs and CD4$^+$ T cells. Additionally, the depletion of pDCs by diphtheria toxin in BDCA2-DTR mice exacerbates TNBS-induced colitis. These findings provide us with valuable insights into the mechanisms by which commensals act on our immune system.

A previous study showed that *B. fragilis* PSA directly interacts with Treg cells via TLR2 to promote immune regulation (Round et al., 2011). Thus, the findings of Dasgupta et al. (2014) raise the question of whether innate pDCs or adaptive Treg cells are more physiologically important for the PSA-induced immune regulatory effects (Figure 1). Interestingly, both studies showed that PSA-mediated activation of pDCs or Treg cells required TLR2. Indeed, TLR2 can mediate immune regulation through Treg cell activation in other contexts (Sutmuller et al., 2006). However, PSA can also induce inflammatory responses in non-pDC antigen-presenting cells through TLR2 (Wang et al., 2006). Although pDCs can promote immune tolerance by inducing Treg cells (Maldonado and von Andrian, 2010), these cells can also evoke antiviral inflammatory responses by producing type I interferons (IFNs). In this regard, pDCs residing in the gut mucosal tissues are thought to be competent for antiviral responses, but PSA stimulation does not induce type I IFN by pDCs. Thus, the PSA-TLR2 axis in pDCs could mediate a novel immunomodulatory pathway that induces Treg cells.

Dasgupta et al. (2014) mainly used bone marrow-derived pDCs. However, bone marrow-derived DCs do not recapitulate the in vivo physiological properties of DCs. The pDCs that reside in the gut-associated lymphoid tissues (GALT) are specialized to induce mucosal immune responses (Tezuka et al., 2011). Therefore, in future studies it would be interesting to analyze whether gut-resident pDCs respond to PSA and induce IL-10-producing Treg cells. It also remains to be determined how intestinal pDCs recognize *B. fragilis* PSA. DCs in the intestinal lamina propria, including CD103$^+$ DCs and CX3CR1$^+$ DCs, have been shown to recognize and take up commensal-derived or lumenal antigens using unique mechanisms (McDole et al., 2012; Rescigno et al., 2001). By contrast, the mechanisms by which intestinal pDCs recognize commensals remain completely uncharacterized. Because pDC have a round-shaped morphology, they are unable to extend their dendrites into the intestinal lumen as CX3CR1$^+$ DCs have been observed to do. To date, no reports have determined whether pDC reside just beneath the epithelial cell layer where they could take up antigens via epithelial cells. The GALT also

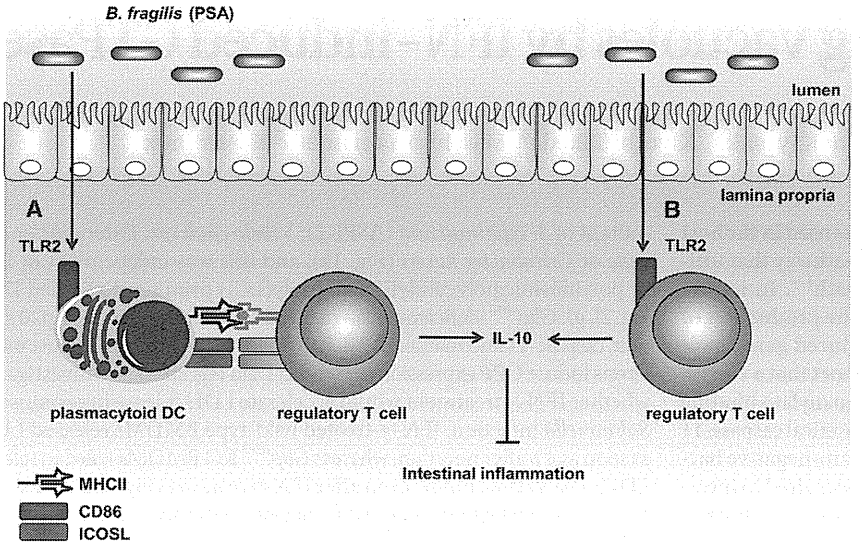

Figure 1. PSA of *B. fragilis* Prevents Intestinal Inflammation by Inducing IL-10 Production in Treg Cells

(A and B) *B. fragilis*-derived PSA enhances induction of TLR2-expressing pDC but not cDC. PSA-activated pDCs induce augmented production of IL-10 in Treg cells via cell-cell interactions, which are mediated by MHC class II, CD86, and ICOSL expressed on the cell surface of pDC. In addition, PSA has been shown to bind to TLR2 on Treg cells, promoting IL-10 production and thereby suppressing intestinal inflammation.

contains pDCs in structures such as Peyer's patches. Therefore, pDCs could possibly recognize commensal-derived antigens in the GALT and then instruct the development of IL-10-producing Treg cells in the gut.

To identify the mechanisms by which other commensal bacteria exert immune regulatory functions, as a community it seems important to study how the dialog between the host immune system and commensal microbes is established. Between the host immune cells and commensals exists the barrier of the intestinal epithelial cell layer. Thus, it remains unclear how pDCs or Treg cells encounter *B. fragilis* PSA in the gut environment. Integrated studies of these three factors—commensals, epithelial barriers, and immune cells—will be needed to gain a better understanding of the mechanisms by which commensal microbes modulate gut immune responses, which can prevent inflammatory bowel diseases.

REFERENCES

Atarashi, K., Tanoue, T., Oshima, K., Suda, W., Nagano, Y., Nishikawa, H., Fukuda, S., Saito, T., Narushima, S., Hase, K., et al. (2013). Nature *500*, 232–236.

Dasgupta, S., Erturk-Hasdemir, D., Ochoa-Repáraz, J., Reinecker, H.-C., and Kasper, D.L. (2014). Cell Host Microbe *15*, 413–423.

Hooper, L.V., Littman, D.R., and Macpherson, A.J. (2012). Science *336*, 1268–1273.

Maldonado, R.A., and von Andrian, U.H. (2010). Adv. Immunol. *108*, 111–165.

Mazmanian, S.K., Round, J.L., and Kasper, D.L. (2008). Nature *453*, 620–625.

McDole, J.R., Wheeler, L.W., McDonald, K.G., Wang, B., Konjufca, V., Knoop, K.A., Newberry, R.D., and Miller, M.J. (2012). Nature *483*, 345–349.

Rescigno, M., Urbano, M., Valzasina, B., Francolini, M., Rotta, G., Bonasio, R., Granucci, F., Kraehenbuhl, J.P., and Ricciardi-Castagnoli, P. (2001). Nat. Immunol. *2*, 361–367.

Round, J.L., Lee, S.M., Li, J., Tran, G., Jabri, B., Chatila, T.A., and Mazmanian, S.K. (2011). Science *332*, 974–977.

Sutmuller, R.P., den Brok, M.H., Kramer, M., Bennink, E.J., Toonen, L.W., Kullberg, B.J., Joosten, L.A., Akira, S., Netea, M.G., and Adema, G.J. (2006). J. Clin. Invest. *116*, 485–494.

Tezuka, H., Abe, Y., Asano, J., Sato, T., Liu, J., Iwata, M., and Ohteki, T. (2011). Immunity *34*, 247–257.

Wang, Q., McLoughlin, R.M., Cobb, B.A., Charrel-Dennis, M., Zaleski, K.J., Golenbock, D., Tzianabos, A.O., and Kasper, D.L. (2006). J. Exp. Med. *203*, 2853–2863.

LETTER

doi:10.1038/nature13157

Caspase-11 activation requires lysis of pathogen-containing vacuoles by IFN-induced GTPases

Etienne Meunier[1], Mathias S. Dick[1]*, Roland F. Dreier[1]*, Nura Schürmann[1], Daniela Kenzelmann Broz[2], Søren Warming[3], Merone Roose-Girma[3], Dirk Bumann[1], Nobuhiko Kayagaki[3], Kiyoshi Takeda[4], Masahiro Yamamoto[4] & Petr Broz[1]

Lipopolysaccharide from Gram-negative bacteria is sensed in the host cell cytoplasm by a non-canonical inflammasome pathway that ultimately results in caspase-11 activation and cell death[1–3]. In mouse macrophages, activation of this pathway requires the production of type-I interferons[4,5], indicating that interferon-induced genes have a critical role in initiating this pathway. Here we report that a cluster of small interferon-inducible GTPases, the so-called guanylate-binding proteins, is required for the full activity of the non-canonical caspase-11 inflammasome during infections with vacuolar Gram-negative bacteria. We show that guanylate-binding proteins are recruited to intracellular bacterial pathogens and are necessary to induce the lysis of the pathogen-containing vacuole. Lysis of the vacuole releases bacteria into the cytosol, thus allowing the detection of their lipopolysaccharide by a yet unknown lipopolysaccharide sensor. Moreover, recognition of the lysed vacuole by the danger sensor galectin-8 initiates the uptake of bacteria into autophagosomes, which results in a reduction of caspase-11 activation. These results indicate that host-mediated lysis of pathogen-containing vacuoles is an essential immune function and is necessary for efficient recognition of pathogens by inflammasome complexes in the cytosol.

Previous studies have reported that induction of caspase-11-dependent cell death by Gram-negative bacteria requires Trif-dependent production of type-I interferons (type-I-IFNs)[4,5] (Extended Data Fig. 1a). Type-I-IFN production is however not required for pro-caspase-11 induction[4,6,7] and is dispensable for caspase-11 activation by transfected lipopolysaccharide (LPS; Extended Data Fig. 1b)[2]. This indicates that interferon-stimulated genes (ISGs) play a major role in activating caspase-11 in response to intracellular bacteria. To investigate which ISGs were involved in activating caspase-11, we used proteomics-based expression analysis to identify proteins that were highly induced following *Salmonella* infection. Among the most strongly upregulated proteins were interferon-induced GTPases, such as the large 65–67 kDa guanylate-binding proteins (GBPs) and small 47 kDa immunity-related GTPases (IRGs) (data not shown). These proteins function in cell-autonomous immunity, that is, mechanisms that allow host cells to kill pathogens or restrict their replication, and have even been associated with the activation of inflammasomes[8–10].

Mice have 11 GBPs, which are highly homologous and are clustered in two genomic loci on chromosomes 3 and 5, respectively[8,11]. Recently, GBPs on chromosome 3 have been shown to restrict the replication of *Toxoplasma gondii* in peritoneal macrophages and mice[11]. We therefore infected bone-marrow-derived macrophages (BMDMs) from Gbp^{chr3} KO mice, which lack GBP1, 2, 3, 5 and 7 (Extended Data Fig. 2a–e), and wild-type littermates with a number of Gram-negative vacuolar pathogens that trigger caspase-11 activation (data not shown)[1,4,5] and determined the activity of the non-canonical inflammasome pathway at 16 h post-infection (Fig. 1a, b). Macrophages from Gbp^{chr3} KO mice showed a significant reduction of cell death (as measured by lactate dehydrogenase (LDH) release) and IL-1β secretion when infected with wild-type *Salmonella typhimurium*, a type three secretion system (T3SS)-deficient mutant of *S. typhimurium* (ΔSPI-2), *Vibrio cholerae*, *Enterobacter cloacae* or *Citrobacter koseri* (Fig. 1a), and this was independent of LPS or polyinosinic:polycytidylic acid (poly(I:C)) priming (Extended Data Fig. 2f, g). Gbp^{chr3}-deficiency also reduced secretion of caspase-1 p20 subunit, caspase-11 and mature IL-1β, IL-18 and IL-1α (Fig. 1b). Because interferons induce GBP expression (Extended Data Fig. 2b, c)[8], we investigated whether IFN-γ treatment would accelerate LDH release in response to *Salmonella* infection. IFN-γ-treated wild-type BMDMs released LDH as soon as 4 h after infection, whereas Gbp^{chr3} KO BMDMs failed to release LDH at early time points even after IFN-γ priming (Fig. 1c), indicating that GBP induction was required for activity of the non-canonical inflammasome pathway.

We next explored whether GBPs play a role in the activation of canonical inflammasomes. LPS-primed wild-type and Gbp^{chr3}-deficient macrophages released comparable levels of LDH and mature IL-1β when infected with logarithmic phase *S. typhimurium*, which exclusively engage the NLRC4 inflammasome via the SPI-1 T3SS (Fig. 1d)[12]. Similarly, Gbp^{chr3}-deficiency did not affect AIM2 inflammasome activation upon poly (deoxyadenylic-deoxythymidylic) acid (poly(dA:dT)) transfection (Fig. 1d). Although GBP5 had been previously linked to NLRP3 activation[9], we did not observe a defect in NLRP3 activation in Gbp^{chr3} KOs (Fig. 1d), possibly owing to different modes of pre-stimulation. These data indicate that GBPs are dispensable for canonical inflammasome activity, but are required for the activation of the non-canonical inflammasome pathway.

To investigate whether GBPs directly mediated the detection of intracellular LPS, we engaged the non-canonical inflammasome by transfecting macrophages with different types of ultra-pure LPS (Fig. 1e). Cytoplasmic LPS triggered LDH release and IL-1β secretion to a similar extent in both wild-type and Gbp^{chr3}-deficient BMDMs, indicating that GBPs were required upstream of LPS sensing and only during bacterial infection. We next investigated if GBPs were required for immune detection of vacuolar or cytosolic bacteria by infecting BMDMs with Δ*sifA S. typhimurium* and *Burkholderia thailandensis*, which rapidly enter the cytosol and activate caspase-11 (ref. 13). Unprimed Gbp^{chr3} KO and wild-type BMDMs responded comparably to these bacteria (Extended Data Fig. 3a–c). Because GBPs might affect this response when pre-induced, we also infected IFN-γ-primed BMDMs with Δ*sifA S. typhimurium* (Extended Data Fig. 3d). IFN-γ-priming indeed resulted in a small difference between wild-type and Gbp^{chr3} KO BMDMs after infection with Δ*sifA Salmonella*, yet not to the extent seen with wild-type *Salmonella* (Fig. 1c), indicating that GBPs mainly participate in the activation of the non-canonical inflammasome by vacuolar bacteria.

Finally, to investigate which GBP controls caspase-11 activation, all 11 murine *Gbp*s were individually knocked down in BMDMs and the cells were infected with flagellin-deficient *Salmonella*, which activate the non-canonical inflammasome but not NLRC4 (Extended Data Fig. 4a and Supplementary Information)[4]. Only knockdown of *Gbp2* resulted in reduced LDH release and IL-1β secretion (Extended Data Fig. 4b–d).

[1]Focal Area Infection Biology, Biozentrum, University of Basel, CH-4056 Basel, Switzerland. [2]Department Biomedicine, University of Basel, CH-4056 Basel, Switzerland. [3]Genentech Inc., South San Francisco, California 94080, USA. [4]Department of Microbiology and Immunology, Osaka University, Yamadaoka, Suita, Osaka 565-0871, Japan.
*These authors contributed equally to this work.

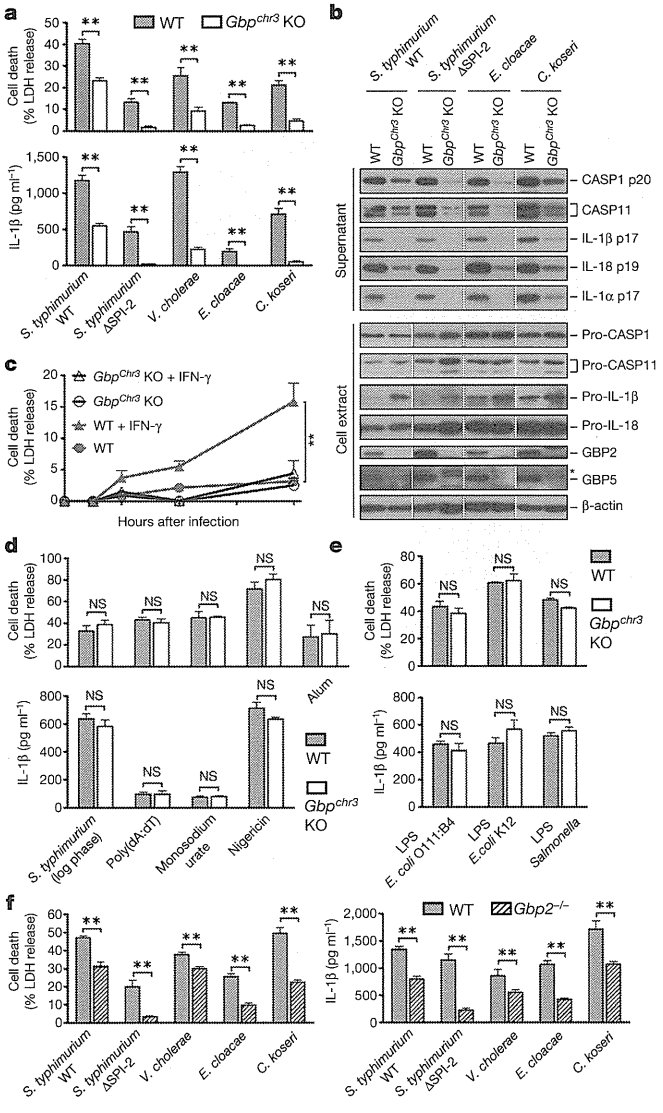

Figure 1 | Caspase-11 activation by intracellular bacterial pathogens requires GBPs. **a**, **b**, LDH release, IL-1β secretion (**a**) and immunoblots for caspase-1, caspase-11, IL-1β, IL-18 and IL-1α (**b**) from unprimed BMDMs infected for 16 h with the indicated bacteria (grown to stationary phase). **c**, Time course measuring LDH release from unprimed or IFN-γ-primed BMDMs infected with *S. typhimurium*. **d**, **e**, LDH release and IL-1β secretion from primed BMDMs infected with SPI-1-expressing logarithmic phase *S. typhimurium*, treated with monosodium urate, alum and nigericin or transfected with poly(dA:dT) and LPS. **f**, LDH release and IL-1β secretion from unprimed wild-type and $Gbp2^{-/-}$ BMDMs infected for 16 h with the indicated bacteria (grown to stationary phase). Graphs show mean and s.d. of quadruplicate wells and data are representative of two (**b**) and three (**a**, **c**–**f**) independent experiments. *Crossreactive band; $^{**}P < 0.01$; NS, not significant (two-tailed *t*-test).

To validate these data we obtained BMDMs from $Gbp2^{-/-}$ mice and wild-type littermates[14] and infected them with vacuolar Gram-negative bacteria. As expected, we observed reduced levels of cell death, cytokine secretion and caspase release in $Gbp2^{-/-}$ BMDMs, indicating attenuated activation of the non-canonical inflammasome (Fig. 1f and Extended Data Fig. 4e), whereas direct LPS sensing or the activation of canonical inflammasomes was not affected (Extended Data Fig. 4f, g). In contrast, *Gbp5*-deficiency did not have any effect on canonical and non-canonical inflammasome activation (Extended Data Fig. 5). Nevertheless, *Gbp2*-deficiency did not reduce caspase-11 activation as markedly as Gbp^{chr3}-deficiency, indicating that whereas caspase-11 activation mainly requires GBP2, other GBPs might also be partially involved.

Reduced numbers of intracellular bacteria could account for low levels of caspase-11 activation in Gbp^{chr3}- and *Gbp2*-deficient macrophages. However, a comparison of wild-type and Gbp^{chr3} KO BMDMs showed that Gbp^{chr3}-deficiency resulted in significantly higher numbers of total and live *Salmonella* per cell (Fig. 2a), consistent with higher colony forming units numbers in Gbp^{chr3} KO BMDMs (Extended Data Fig. 6). In addition, fluorescence-activated cell sorting (FACS)-based analysis of dead (mCherry-negative, $FITC^+$) and live (mCherry-positive, $FITC^+$) *Salmonella* at 16 h post-infection found significantly fewer dead bacteria (~20%) in GBP^{chr3} KO and $Gbp2^{-/-}$ BMDMs when compared to wild-type BMDMs (>30%) (Fig. 2b). Importantly, bacterial killing in $Casp11^{-/-}$ BMDMs was comparable to wild-type BMDMs, indicating that the control of bacterial replication was directly linked to GBP function and not to the activation of the non-canonical inflammasome (Fig. 2b). In conclusion, we show that GBPs control bacterial replication on a cell-autonomous level, which is consistent with a previous report that GBP1 partially restricts *Mycobacterium bovis* and *Listeria monocytogenes* replication[10].

Restricting bacterial replication has been proposed to require the association of GBPs with pathogen-containing vacuoles and the recruitment of antimicrobial factors[8]. We therefore investigated whether GBPs targeted intracellular Gram-negative bacteria. Indeed, GBP2 could be detected on intracellular bacteria within hours after infection (Fig. 2c). Very little GBP-positive bacteria were detected in $Stat1^{-/-}$ BMDMs, which do not respond to type-I- and type-II-IFNs and largely failed to induce GBP expression (data not shown). Remarkably, GBP-positive *Salmonella* seemed to have lost mCherry expression (Fig. 2c), indicating that these bacteria were dead. To determine whether GBPs are recruited to dead bacteria we infected BMDMs with *Salmonella* killed by heat, paraformaldehyde or 70% ethanol treatment, yet only live *Salmonella* acquired GBP staining and activated the inflammasome (Fig. 2d). To examine this mechanism *in vivo*, we immunostained spleen tissue sections of mice infected with *Salmonella* for GBPs. Indeed, GBPs could also be found associated with approximately 20% of bacteria *in vivo*, and a significantly higher proportion of these bacteria were dead, based on the loss of mCherry expression (Fig. 2e–g). Furthermore, treatment with IFN-γ-neutralizing antibodies reduced the percentage of GBP-positive bacteria (Fig. 2f), consistent with reports that IFN-γ controls *Salmonella* replication *in vivo*[15,16]. Taken together, these results indicated that GBPs either kill bacteria directly or control an antimicrobial effector pathway, and raised the interesting possibility that GBP-mediated killing of bacteria might result in the release of LPS and caspase-11 activation[2,3].

To identify the antimicrobial effector pathway that is controlled by GBPs we first examined the role of free radicals[8]. Although GBP7 was reported to be required for reactive oxygen species (ROS) production and to interact with the phagosome oxidase complex[10], we did not find any role for ROS or NO production in caspase-11 activation (Extended Data Fig. 7). Furthermore, GBPs were also proposed to recruit components of the autophagy machinery to pathogen-containing vacuoles (PCVs), possibly resulting in bacterial killing within autophagosomes[8,10]. Indeed, many GBP-positive *S. typhimurium*, *E. cloacae* and *C. koseri* co-stained for the commonly used autophagy marker LC3 (Fig. 3a and Extended Data Fig. 8a). Recruitment of LC3 to intracellular *Salmonella* was partially GBP-dependent, because we found significantly lower numbers of LC3-positive *Salmonella* in Gbp^{chr3} KO compared to wild-type macrophages (Fig. 3b, c). Therefore, we speculated that autophagy-mediated killing might result in the release of LPS from bacteria and caspase-11 activation. Unexpectedly, however, pharmacological inhibition of autophagy with 3-methyladenine (3-MA) resulted in significantly higher levels of LDH release, IL-1β secretion and caspase-1/caspase-11 activation in macrophages infected with *S. typhimurium*, *E. cloacae* or *C. koseri* (Fig. 3d, e), indicating increased activation of the non-canonical inflammasome. Consistently, cell death was still caspase-11-dependent because $Casp11^{-/-}$ BMDMs did not release LDH when treated with 3-MA and infected with Gram-negative bacteria (Fig. 3f). Direct activation of caspase-11 by LPS transfection was independent of

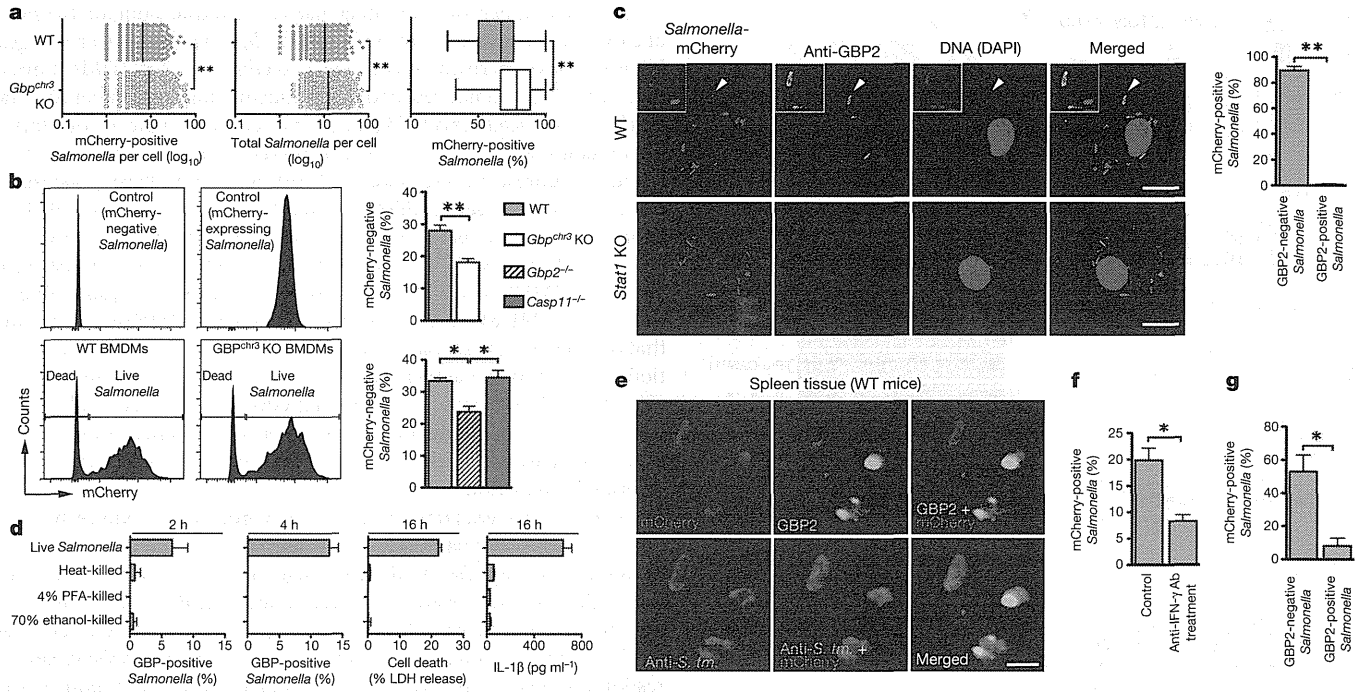

Figure 2 | GBPs control bacterial replication. **a**, **b**, Quantification of live (mCherry-positive) and dead (mCherry-negative) *S. typhimurium* per cell by immunofluorescence (**a**) or as percent of total by flow-cytometry (**b**) in unprimed BMDMs at 16 h post-infection. **c**, Immunostaining for GBP2 and quantification of live and dead *Salmonella* at 4 h post-infection. Arrowheads, bacteria shown in insets. **d**, Quantification of GBP-positive bacteria, LDH release and IL-1β secretion at indicated time points from BMDMs infected with *Salmonella*, live or killed by different means. **e**, Immunohistochemistry for GBP2 and *Salmonella* on spleen tissue from *Salmonella* (mCherry-positive)-infected mice (representative of $n = 3$ per group). *S. tm.*, *S. typhimurium*. **f**, **g**, Quantification of GBP-positive *Salmonella* in anti-IFN-γ-treated or control animals (**f**) and live and dead bacteria among GBP2-negative/-positive *Salmonella* (**g**) ($n = 3$ per group). Scale bars, 10 μm (**c**), 1 μm (**e**). Graphs show mean and 5–95 percentile (box plots) or s.d. of technical triplicates, and data are representative of three independent experiments. $^*P < 0.05$, $^{**}P < 0.01$ (two-tailed *t*-test).

autophagy (Fig. 3g), indicating that autophagy only counteracts non-canonical inflammasome activation during bacterial infections. To further confirm our data, we infected *Atg5*$^{-/-}$ BMDMs with *S. typhimurium* and we also observed significantly higher levels of non-canonical inflammasome activation compared to wild-type BMDMs (Fig. 3h, i). Taken together, these results indicated that, although GBPs promoted the uptake of bacteria into autophagosomes, autophagy actually counteracted caspase-11 activation. Thus, GBP-dependent LPS detection occurs before bacteria are targeted to autophagosomes.

A possible explanation could be that autophagy sequesters bacteria that had escaped from the vacuole, and thus prevents further LPS release into the cytosol. Recently, the cytosolic danger receptor galectin-8 was reported to function as a marker for lysed vacuoles. Galectin-8 binds β-galactosides, which are normally found on the inner leaflet of the vacuolar membrane and get exposed to the cytosol upon vacuolar lysis[17]. Indeed, quantification of galectin-8-positive *Salmonella* showed that significantly fewer bacteria were targeted by galectin-8 in *Gbp*^{chr3} KO BMDMs than in wild-type macrophages (Fig. 4a). Because galectin-8 colocalized with GBP- and LC3-positive *Salmonella* (Fig. 4b, c), we speculated that GBPs promote LC3 recruitment through galectin-8. Consistently, we found lower levels of galectin-8-positive *Salmonella* among LC3-positive *Salmonella* in *Gbp*^{chr3} KO compared to wild-type BMDMs (Fig. 4d). Galectin-8 interacts with the autophagy adaptor protein NDP52, which in humans contains binding sites for galectin-8, ubiquitin and LC3[18]. In line with a role for NDP52 in linking galectin-8 to LC3, murine NDP52 colocalized with galectin-8 on intracellular *Salmonella* (Extended Data Fig. 8b). Targeting of *Salmonella* to autophagosomes might also involve other autophagy cargo adaptors, because p62 was associated with the majority of LC3-positive bacteria, yet this was independent of GBPs (Extended Data Fig. 8c, d). Altogether, these results suggested that GBPs might promote the lysis of vacuoles or help to recruit galectin-8 to lysed vacuoles.

To confirm a direct role of GBPs in vacuolar lysis, we adapted a phagosome integrity assay based on differential permeabilization with digitonin (Extended Data Fig. 9). Comparing wild-type and *GBP*^{chr3} KO BMDMs, we found significantly lower numbers of cytosolic (FITC$^+$) *S. typhimurium* in *Gbp*^{chr3}-deficient cells (Fig. 4e, f). Similarly, *Gbp2*$^{-/-}$ BMDMs also harboured fewer cytosolic *S. typhimurium* compared to BMDMs from wild-type littermates (Fig. 4g). In contrast, we did not find a defect in cytosolic localization between wild-type and *Gbp*^{chr3} KO BMDMs infected with the specialized cytosolic pathogen *Shigella flexneri*, which uses its T3SS to destabilize the phagosome and escape into the cytoplasm (Fig. 4h)[19]. Although we cannot exclude that GBPs might also be involved in the recruitment or assembly of the non-canonical inflammasome, these results indicate that GBPs, in particular GBP2, directly promote the destruction of vacuoles.

In conclusion, our data demonstrate that host-induced destruction of PCVs or phagosomes is an essential immune function and assures recognition of vacuolar bacteria by cytosolic innate immune sensors (Extended Data Fig. 10). Additional studies are required to determine how GBPs distinguish 'self' and 'non-self' membranes and by which mechanism phagosomes are lysed. In mice, this might involve the IRGM proteins that can act as GDI (guanine nucleotide dissociation inhibitor) and inhibit IRG and GBP activity. Absence of IRGMs results in mislocalization of both IRGs and GBPs and even in degradation of lipid droplets[20–22], supporting a model in which IRGM proteins would protect 'self'-vacuoles from being targeted by host IRGs and GBPs[23]. Because both commensals and pathogens activate caspase-11 (ref. 1), it can be assumed that GBPs are not specific towards pathogens but are a general innate immune response against bacteria trapped in the phagosomes of macrophages. Finally, given the important role of LPS-induced caspase-11 activation in septic shock[1–3], pharmaceutical targeting of the above-described pathways might be used to modulate inflammation during bacterial sepsis.

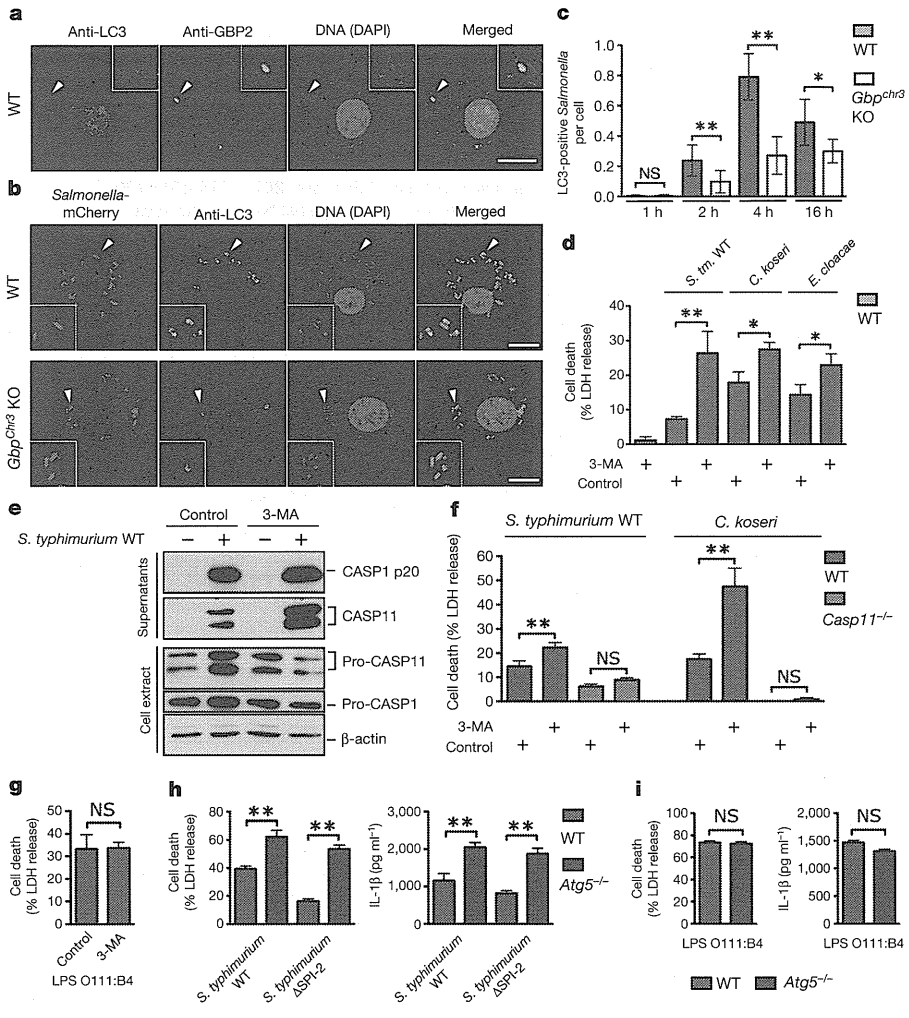

Figure 3 | Autophagy reduces caspase-11 activation. **a**, **b**, Unprimed BMDMs infected with *S. typhimurium* for 4 h and immunostained for LC3 and GBP2. Arrowheads, bacteria shown in insets. Scale bars, 10 μm. **c**, Quantification of results from **b**. **d**–**g**, LDH release and immunoblots for caspase-1 and caspase-11 from BMDMs infected for 16 h or transfected with LPS in presence or absence of 3-methyladenine (3-MA). **h**, **i**, LDH release and IL-1β secretion from BMDMs infected for 16 h or transfected with LPS. Graphs show mean and s.d. of quadruplicate wells and data are representative of two (**e**, **i**) and three (**a**–**d**, **f**–**h**) independent experiments. $*P < 0.05$, $**P < 0.01$; NS, not significant (two-tailed *t*-test).

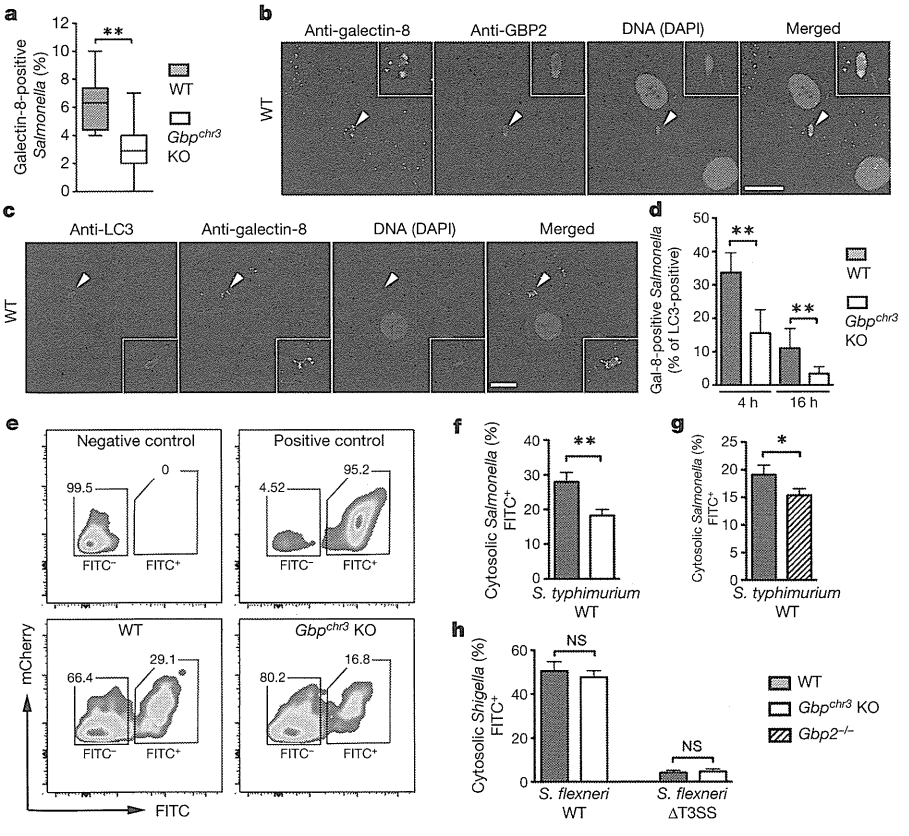

Figure 4 | GBP-mediated lysis of the PCV releases *Salmonella* into the cytosol. **a**, Quantification of galectin-8-positive *Salmonella* in unprimed BMDMs at 4 h post-infection. **b**, **c**, Unprimed BMDMs infected with *S. typhimurium* for 4 h and immunostained for galectin-8, GBP2 and LC3. Arrowheads, bacteria shown in insets. Scale bars, 10 μm. **d**, Quantification of galectin-8/LC3-double-positive *Salmonella* at indicated time points post-infection. **e**–**h**, Quantification of cytosolic and vacuolar bacteria by flow cytometry in BMDMs infected with mCherry-positive *S. typhimurium* (**e**–**g**) or *S. flexneri* (**h**, wild-type or ΔT3SS) for 4 h. Graphs show mean and s.d. or 5–95 percentile (Box plots) of technical triplicates. Data are representative of 2 (**g**, **h**), 3 (**a**–**d**) and 4 (**e**, **f**) independent experiments. $*P < 0.05$, $**P < 0.01$ (two-tailed *t*-test).

METHODS SUMMARY

BMDMs were cultured and seeded for infections as described previously[4]. Priming was done overnight with PAM3CSK4 (1 μg ml^{-1}), LPS O111:B4 (0.1 μg ml^{-1}), murine IFN-β or murine IFN-γ (1 unit per μl). *S. typhimurium*, *S. flexneri*, *V. cholerae*, *E. cloacae*, *C. koseri* and *B. thailandensis* were grown overnight in LB or TSB medium at 37 °C with aeration. Bacteria were diluted in fresh pre-warmed macrophage medium and added to the macrophages at a multiplicity of infection (m.o.i.) of 100:1 for measurements of caspase-11 and caspase-1 activity or 10:1 for all other assays. For assaying NLRC4 activation, *Salmonella* were subcultured for 4 h to induce SPI-1 T3SS expression before infection (m.o.i. 20:1). *S. flexneri* were subcultured for 3 h to induce T3SS expression before infection (m.o.i. 30:1). When required, apocynin, L-NG-nitroarginine methyl ester (L-NAME), 3-methyladenine or vehicle controls were added 30 min before infection. Plates were centrifuged for 15 min at 500*g* to synchronize the infection and placed at 37 °C for 1 h. Next, 100 μg ml^{-1} gentamycin was added to kill extracellular bacteria. After 1 h incubation, the cells were washed once with DMEM and given fresh macrophage medium containing 10 μg ml^{-1} gentamicin for the remainder of the infection. Transfection with poly(dA:dT) or MSU, alum or nigericin treatment was done as described previously[2] or as indicated. All animal experiments were approved and performed according to local guidelines. Female BALB/c mice (10–14 weeks old) were infected intravenously with *Salmonella* (1,000 c.f.u.) and euthanized 4–5 days later. For antibody injections, mice received on day 3 two intraperitoneal injections of 200 μl PBS containing 0.2 mg anti-IFN-γ monoclonal or 0.2 mg rat IgG1, κ isotype control antibody.

Online Content Any additional Methods, Extended Data display items and Source Data are available in the online version of the paper; references unique to these sections appear only in the online paper.

Received 31 October 2013; accepted 14 February 2014.
Published online 16 April 2014.

1. Kayagaki, N. *et al.* Non-canonical inflammasome activation targets caspase-11. *Nature* **479,** 117–121 (2011).
2. Kayagaki, N. *et al.* Noncanonical inflammasome activation by intracellular LPS independent of TLR4. *Science* **341,** 1246–1249 (2013).
3. Hagar, J. A., Powell, D. A., Aachoui, Y., Ernst, R. K. & Miao, E. A. Cytoplasmic LPS activates caspase-11: implications in TLR4-independent endotoxic shock. *Science* **341,** 1250–1253 (2013).
4. Broz, P. *et al.* Caspase-11 increases susceptibility to *Salmonella* infection in the absence of caspase-1. *Nature* **490,** 288–291 (2012).
5. Rathinam, V. A. *et al.* TRIF licenses caspase-11-dependent NLRP3 inflammasome activation by Gram-negative bacteria. *Cell* **150,** 606–619 (2012).
6. Case, C. L. *et al.* Caspase-11 stimulates rapid flagellin-independent pyroptosis in response to *Legionella pneumophila*. *Proc. Natl Acad. Sci. USA* **110,** 1851–1856 (2013).
7. Casson, C. N. *et al.* Caspase-11 activation in response to bacterial secretion systems that access the host cytosol. *PLoS Pathog.* **9,** e1003400 (2013).
8. MacMicking, J. D. Interferon-inducible effector mechanisms in cell-autonomous immunity. *Nature Rev. Immunol.* **12,** 367–382 (2012).
9. Shenoy, A. R. *et al.* GBP5 promotes NLRP3 inflammasome assembly and immunity in mammals. *Science* **336,** 481–485 (2012).
10. Kim, B. H. *et al.* A family of IFN-gamma-inducible 65-kD GTPases protects against bacterial infection. *Science* **332,** 717–721 (2011).
11. Yamamoto, M. *et al.* A cluster of interferon-gamma-inducible p65 GTPases plays a critical role in host defense against *Toxoplasma gondii*. *Immunity* **37,** 302–313 (2012).
12. Broz, P. *et al.* Redundant roles for inflammasome receptors NLRP3 and NLRC4 in host defense against *Salmonella*. *J. Exp. Med.* **207,** 1745–1755 (2010).
13. Aachoui, Y. *et al.* Caspase-11 protects against bacteria that escape the vacuole. *Science* **339,** 975–978 (2013).
14. Degrandi, D. *et al.* Murine guanylate binding protein 2 (mGBP2) controls *Toxoplasma gondii* replication. *Proc. Natl Acad. Sci. USA* **110,** 294–299 (2013).
15. VanCott, J. L. *et al.* Regulation of host immune responses by modification of *Salmonella* virulence genes. *Nature Med.* **4,** 1247–1252 (1998).
16. Burton, N. A. *et al.* Disparate impact of oxidative host defenses determines the fate of *Salmonella* during systemic infection in mice. *Cell Host Microbe* **15,** 72–83 (2014).
17. Thurston, T. L., Wandel, M. P., von Muhlinen, N., Foeglein, A. & Randow, F. Galectin 8 targets damaged vesicles for autophagy to defend cells against bacterial invasion. *Nature* **482,** 414–418 (2012).
18. Deretic, V., Saitoh, T. & Akira, S. Autophagy in infection, inflammation and immunity. *Nature Rev. Immunol.* **13,** 722–737 (2013).
19. Paetzold, S., Lourido, S., Raupach, B. & Zychlinsky, A. *Shigella flexneri* phagosomal escape is independent of invasion. *Infect. Immun.* **75,** 4826–4830 (2007).
20. Hunn, J. P. *et al.* Regulatory interactions between IRG resistance GTPases in the cellular response to *Toxoplasma gondii*. *EMBO J.* **27,** 2495–2509 (2008).
21. Traver, M. K. *et al.* Immunity-related GTPase M (IRGM) proteins influence the localization of guanylate-binding protein 2 (GBP2) by modulating macroautophagy. *J. Biol. Chem.* **286,** 30471–30480 (2011).
22. Haldar, A. K. *et al.* IRG and GBP host resistance factors target aberrant, "non-self" vacuoles characterized by the missing of "self" IRGM proteins. *PLoS Pathog.* **9,** e1003414 (2013).
23. Coers, J. Self and non-self discrimination of intracellular membranes by the innate immune system. *PLoS Pathog.* **9,** e1003538 (2013).

Supplementary Information is available in the online version of the paper.

Acknowledgements We thank N. Mizushima and S. Virgin for *Atg5*-deficient BMDMs, K. Pfeffer for *Gbp2*-deficient BMDMs, J. Frey for *B. thailandensis*, the Biozentrum Proteomics and Imaging Core Facilities for technical assistance, K. Anderson, T. Soukup, R. Schwingendorf, J. C. Cox, V. M. Dixit for reagents and N. Personnic for discussions. This work was supported by an SNSF Professorship PP00P3_139120/1, University of Basel project grant ID2153162 to P.B. and a Marie Heim-Voegtlin Fellowship 145516 to D.K.B.

Author Contributions E.M. and P.B. designed the study and wrote the manuscript. E.M., R.F.D., M.S.D., N.S. and P.B. performed the experiments and analysed data; D.K.B., D.B., S.W., M.R.-G., N.K., M.Y. and K.T. contributed reagents.

Author Information Reprints and permissions information is available at www.nature.com/reprints. The authors declare no competing financial interests. Readers are welcome to comment on the online version of the paper. Correspondence and requests for materials should be addressed to P.B. (petr.broz@unibas.ch).

METHODS

Bacterial strains and plasmids. *Salmonella enterica* serovar Typhimurium (*S. typhimurium*) SL1344 and congenic mutants were published before[12]. Other bacterial strains used were *Shigella flexneri, Vibrio cholerae, Enterobacter cloacae, Citrobacter koseri* and *Burkholderia thailandensis* ATCC700388.

Mice. *Gbp*^{chr3} KO, *Gbp2*$^{-/-}$, *Atg5*$^{fl/fl}$-Lyz-Cre, *Cybb*$^{-/-}$ (gp91^{phox}), *Casp1*$^{-/-}$/*Casp11*$^{-/-}$ (a.k.a caspase-1 knockout), *Casp11*$^{-/-}$ and *Casp1*$^{-/-}$ (*Casp1*$^{-/-}$/*Casp11*^{tg}) mice have been previously described[1,11,14,24,25]. Mice were bred in the animal facilities of the University of Basel, Genentech Inc., Heinrich-Heine-University Duesseldorf or the University of Osaka. Generation of mice with *Gbp5* KO alleles by zinc finger nuclease (ZFN) technology: A ZFN pair was obtained from Sigma-Aldrich (SAGE Labs). The ZFN pair recognizes a sequence in mouse *Gbp5* exon 2 (cut site is underlined): 5′-TGCCATCACACAGCCAGTGGTGGTAGCCATTGTGG GT-3′. ZFN mRNA and a donor plasmid harbouring a 10-bp deletion in *Gbp5* exon 2 was co-microinjected into C57BL/6N zygotes using established procedures. One male founder carrying the 10-bp deletion was obtained by homologous recombination (10-bp deletion is underlined): 5′-TGCCATCACACAGCCAGTG GTGGTGGTAGCCATTGTGGGT-3. This founder was bred with C57BL/6N females to generate heterozygous progeny for subsequent intercrossing. Two founders (a male and a female) carrying identical 1-bp deletions were obtained by non-homologous end-joining (deleted bp is underlined): 5′-TGCCATCACACAGCCAGTGGTGG TGGTAGCCATTGTGGGT-3. These two founders were intercrossed to directly generate homozygous progeny. Both the 10-bp (designated KO line 1) and 1 bp (designated KO line 2) deletions lead to frameshifts and premature stop codons in *Gbp5* exon 2.

Animal infection. All animal experiments were approved (license 2239, Kantonales Veterinäramt Basel-Stadt) and performed according to local guidelines (Tierschutz-Verordnung, Basel-Stadt) and the Swiss animal protection law (Tierschutz-Gesetz). Female BALB/c mice (10–14 weeks old) were infected intravenously with mCherry-positive *Salmonella* (1,000 c.f.u.) and euthanized 4–5 days later. For antibody injections, mice ($n = 3$ per group) received on day 3 two intraperitoneal injections of 200 µl PBS containing 0.2 mg anti-IFN-γ monoclonal antibody (Clone XMG1.2, BioLegend) or 0.2 mg rat IgG1, κ isotype control antibody (clone RTK2071, BioLegend). No randomization or blinding was performed.

Cell culture and infections. BMDMs were differentiated in DMEM (Invitrogen) with 10% v/v FCS (Thermo Fisher Scientific), 10% MCSF (L929 cell supernatant), 10 mM HEPES (Invitrogen), and nonessential amino acids (Invitrogen). 1 day before infection, macrophages were seeded into 6-, 24-, or 96-well plates at a density of 1.25×10^6, 2.5×10^5, or 5×10^4 per well. If required macrophages were pre-stimulated with PAM3CSK4, LPS O111:B4 (InvivoGen), mIFN-β or mIFN-γ (eBioscience). For infections with *S. typhimurium, V. cholerae, E. cloacae, C. koseri* and *B. thailandensis*, bacteria were grown overnight in LB or TSB at 37 °C with aeration. The bacteria were diluted in fresh pre-warmed macrophage medium and added to the macrophages at an multiplicity of infection (m.o.i.) of 100:1 for measurements of caspase-11 and caspase-1 activity or 10:1 for all other assays. For assaying *Salmonella*-induced NLRC4 activation, *Salmonella* were subcultured for 4 h before infection to induce SPI-1 T3SS and flagellin expression. *S. flexneri* were cultured overnight in TSB medium and subcultured for 3 h before infection to induce T3SS expression. IFN-γ-primed BMDMs (to induce GBP expression) were infected with m.o.i. of 30:1 with *S. flexneri* for FACS analysis. When required, chemical reagents, Apocynin (Sigma Aldrich, 100µM), L-NG-nitroarginine methyl ester (L-NAME; Sigma Aldrich, 100 µM) and 3-methyladenine (Sigma Aldrich, 5 mM) were added 30 min before infection. The plates were centrifuged for 15 min at 500 *g* to ensure comparable adhesion of the bacteria to the cells and placed at 37 °C for 60 min. Next, 100 µg ml^{-1} gentamycin (Invitrogen) was added to kill extracellular bacteria. After a 60-min incubation, the cells were washed once with DMEM and given fresh macrophage medium containing 10 µg ml^{-1} gentamicin for the remainder of the infection. For infections with killed bacteria, *Salmonella* were grown as above. Shortly before the infection, bacteria were left untreated or incubated for 30 min at 95 °C, in 4% paraformaldehyde or in 70% ethanol. Following the treatment, bacteria were washed with PBS and prepared for infections as outlined above. The effectiveness of the killing procedures was verified by plating serial dilutions. Transfection with poly(dA:dT) or treatment with MSU, alum or nigericin was done as described previously[2] or as indicated.

siRNA knockdown. Gene knockdown was done using GenMute (SignaGen) and siRNA pools (siGenome, Dharmacon). Briefly, wild-type BMDMs were seeded into 24-, or 96-well plates at a density of 1.5×10^5 or 3×10^4 per well. siRNA complexes were prepared at 25 nM siRNA in 1× GenMute Buffer according to the manufacturer's instructions for forward knockdowns. siRNA complexes were mixed with BMDM medium and added onto the cells. BMDMs were infected with *S. typhimurium* at an m.o.i. of 100:1 after 56 h of knockdown and analysed for inflammasome activation as outlined below. siRNA pools included: *Casp11* (that is, *Casp4*) (M-042432-01), *Gbp1* (M-040198-01), *Gbp2* (M-040199-00), *Gbp3* (M-063076-01), *Gbp4* (M-047506-01), *Gbp5* (M-054703-01), *Gbp6* (M-041286-01), *Gbp7* (M-061204-01), *Gbp8* (M-059726-01), *Gbp9* (M-052281-01), *Gbp10* (M-073912-00), *Gbp11* (M-079932-00) and NT (non-targeting) pool 2 (D-001206-14). See Supplementary information for sequences.

LPS transfection. Macrophages were seeded as described above. Cells were pre-stimulated with 10 ug ml^{-1} of PAM3CSK4 for 4 h in Opti-MEM and transfected for 16 h with ultrapure LPS *E. coli* O111:B4, ultrapure LPS *E. coli* K12 or ultrapure LPS *Salmonella minnesota* (InvivoGen) in complex with FuGeneHD (Promega) as described previously[2].

Cytokine and LDH release measurement. IL-1β and tumour necrosis factor (TNF)-α was measured by ELISA (eBioscience). LDH was measured using LDH Cytotoxicity Detection Kit (Clontech). To normalize for spontaneous lysis, the percentage of LDH release was calculated as follows: (LDH infected − LDH uninfected)/(LDH total lysis − LDH uninfected)*100.

Western blotting. Western blotting was done as described before[4]. Antibodies used were rat anti-mouse caspase-1 antibody (1:1,000; 4B4; Genentech), rat anti-mouse caspase-11 (1:500; 17D9; Sigma), rabbit anti-IL-1α (1:1,000; ab109555; Abcam), rabbit anti-IL-18 (1:500; 5180R; Biovision), goat anti-mouse IL-1β antibody (1:500; AF-401-NA; R&D Systems) and rabbit anti-GBP2 and rabbit anti-GBP5 (1:1,000; 11854-1-AP/13220-1-AP; Proteintech). Cell lysates were probed with anti-β-actin antibody (Sigma) at 1:2,000.

Statistical analysis. Statistical data analysis was done using Prism 5.0a (GraphPad Software, Inc.). To evaluate the differences between two groups (cell death, cytokine release, FACS, CFU and immunofluorescence-based counts) the two-tailed *t*-test was used. In figures NS indicates 'not significant', *P* values are given in figure legends.

Immunofluorescence. Macrophages were seeded on glass coverslips and infected as described above. At the desired time points cells were washed 3× with PBS and fixed with 4% paraformaldehyde for 15 min at 37 °C. Following fixation coverslips were washed and the fixative was quenched with 0.1 M glycine for 10 min at room temperature. Coverslips were stained with primary antibodies at 4 °C for 16 h, washed 4× with PBS, incubated for 1 h with appropriate secondary antibodies at room temperature (1:500, AlexaFluor, Invitrogen), washed 4× with PBS and mounted on glass slides with Vectashield containing 4′,6-diamidino-2-phenylindole (DAPI) (Vector Labs). Antibodies used were rabbit anti-LC3 (1:1,000; NB600-1384, Novus), mouse anti-LC3 (1:100, 2G6, NanoTools), guinea-pig anti-p62 (1:100, GP62-C, Progen), goat anti-*Salmonella* (1:500, CSA-1 and CSA-1-FITC, KPL), mouse anti-galectin-8 (1:1,000, G5671, Sigma), goat anti-galectin-8 (1:100, AF1305, R&D), rabbit anti-Optineurin (1:100, ab23666, Abcam), rabbit anti-NDP52 (1:100, D01, Abnova), anti-PDI (1:100, ADI-SPA-890, Enzo Lifesciences), anti-Calnexin (1:100, ADI-SPA-860-D, Enzo Lifesciences), goat anti-GBP1-5 (1:100, sc-166960, Santa Cruz Biotech), rabbit anti-GBP2 and rabbit anti-GBP5 (1:100; 11854-1-AP/13220-1-AP; Proteintech). Coverslips were imaged on a Zeiss LSM700 or a Leica SP8 at ×63 magnification. Colocalization studies were performed as blinded experiments, with in general a minimum count of 100 bacteria per coverslip and performed in triplicate. Immunofluorescence based counts of live (mCherry$^+$/FITC$^+$) and dead (mCherry$^-$/FITC$^+$) bacteria were done as blinded experiment on *z* stacks taken from 15 random fields in three biological replicates, with a total of approximately 10,000 bacteria counted.

Immunohistochemistry. Cryosections were blocked in 1% blocking reagent (Invitrogen) and 2% mouse serum (Invitrogen) in TBST (0.05% Tween in 1× TBS pH 7.4), and stained with primary and secondary antibodies (goat anti-CSA1; 1:500; 01-91-99-MG; KPL and anti-GBP2; 1:100; 11854-1-AP; Proteintech). Secondary antibodies included Santa Cruz Biotech sc-362245 and Molecular Probes A21206, A21445 and A21469.

ROS assay. Measurement of oxygen-dependent respiratory burst of BMDMs was performed by chemiluminescence in the presence of 5-amino-2,3-dihydro-1,4-phtalazinedione (luminol, Sigma Aldrich, 66 µM) using a thermostatically (37 °C) controlled luminometer. Both oxygen and nitrogen species were detected ($O_2^{\bullet -}$, $ONOO^-$, $OH^{\bullet}$). Chemiluminescence generation was monitored every minute for 1 h after IFN-γ (100 U ml^{-1}) and/or *Salmonella* challenge and expressed as counts per minute.

NO assay. Nitrite production was measured by the Griess assay as previously described[26]. Briefly, in 96-well plates, BMDMs were infected as described above in presence or absence of IFN-γ or IL-1β for 16 h. Supernatants were mixed 1:1 with 2.5% phosphoric acid solution containing 1% sulfanilamide and 0.1% naphthylenediamine. After 30 min incubation at room temperature, the nitrite concentration was determined by measuring absorbance at 550 nm. Sodium nitrite (Sigma) was used as a standard to determine nitrite concentrations in the cell-free medium.

Digitonin assay. For flow-cytometry-based quantification of cytoplasmic and vacuolar bacteria, macrophages were infected with mCherry$^+$ *S. typhimurium* or mCherry$^+$ *S. flexneri* as described above. At the desired time point, cells were washed 3× with KHM buffer (110 mM potassium acetate, 20 mM HEPES, 2 mM $MgCl_2$,

pH 7.3) and incubated for 1 min in KHM buffer with 150 μg ml^{-1} digitonin (Sigma). Cells were immediately washed 2× with KHM buffer and then stained for 12 min with anti-*Salmonella*-FITC (1:500, CSA-1, KPL) or anti-*Shigella* (1:100, BP1064, Acris) in KHM buffer with 2% BSA. Secondary antibodies used for *S. flexneri* staining were: anti-Rabbit-488 (1:500, Invitrogen). Cells were washed 3× with PBS and lysed in PBS with 0.1% Triton-X (Sigma) and analysed on a FACS-Canto-II. Controls were included in every assay and are described in (Extended Data Fig. 9).

Live/dead analysis by FACS. Infection of macrophages was performed using mCherry^{+} bacteria as described above. At 16 h post-infection cells were washed and lysed with PBS solution containing 0.1% Triton X-100 (Sigma Aldrich) to release intracellular bacteria. *Salmonella* were counterstained using an anti-*Salmonella* antibody (CSA-1, KPL) and analysed using a FACS Canto-II for fluorescence intensities in FL-1 and FL-2 channels. Data were analysed with FlowJo 10.0.6 software. The gate was set for the bacterial population based on the FSC/SSC and the anti-*Salmonella* staining (CSA-1-FITC, KPL). Controls included live mCherry-expressing and mCherry-negative *Salmonella* stained with anti-*Salmonella* antibodies (CSA-1, KPL).

24. Mariathasan, S. *et al.* Differential activation of the inflammasome by caspase-1 adaptors ASC and Ipaf. *Nature* **430,** 213–218 (2004).
25. Zhao, Z. *et al.* Autophagosome-independent essential function for the autophagy protein Atg5 in cellular immunity to intracellular pathogens. *Cell Host Microbe* **4,** 458–469 (2008).
26. Lima-Junior, D. S. *et al.* Inflammasome-derived IL-1β production induces nitric oxide-mediated resistance to *Leishmania*. *Nature Med.* **19,** 909–915 (2013).

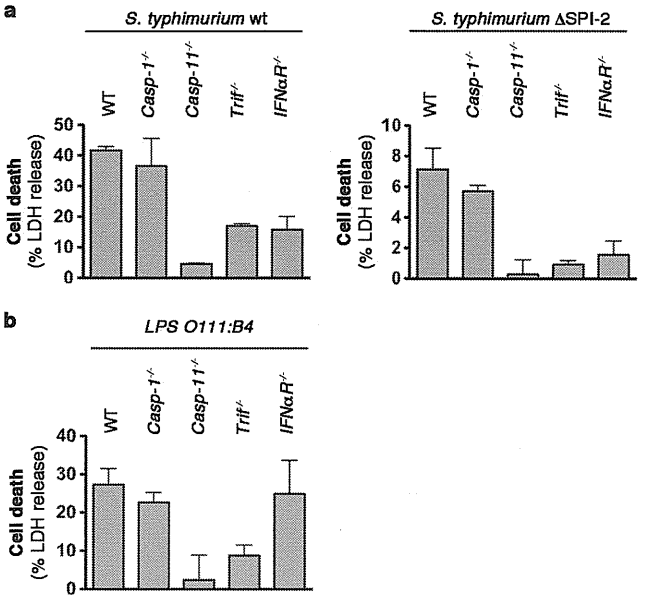

Extended Data Figure 1 | Type-I-interferon signalling is required to induce caspase-11-dependent cell death in response to bacterial infection, but not in response to LPS transfection. **a**, LDH release from unprimed BMDMs infected for 16 h with wild-type (WT) *S. typhimurium* or ΔSPI-2 *S. typhimurium* grown to stationary phase. **b**, LDH release from primed BMDMs transfected with LPS O111:B4. Graphs show the mean and s.d. of quadruplicate wells and are representative of three independent experiments.

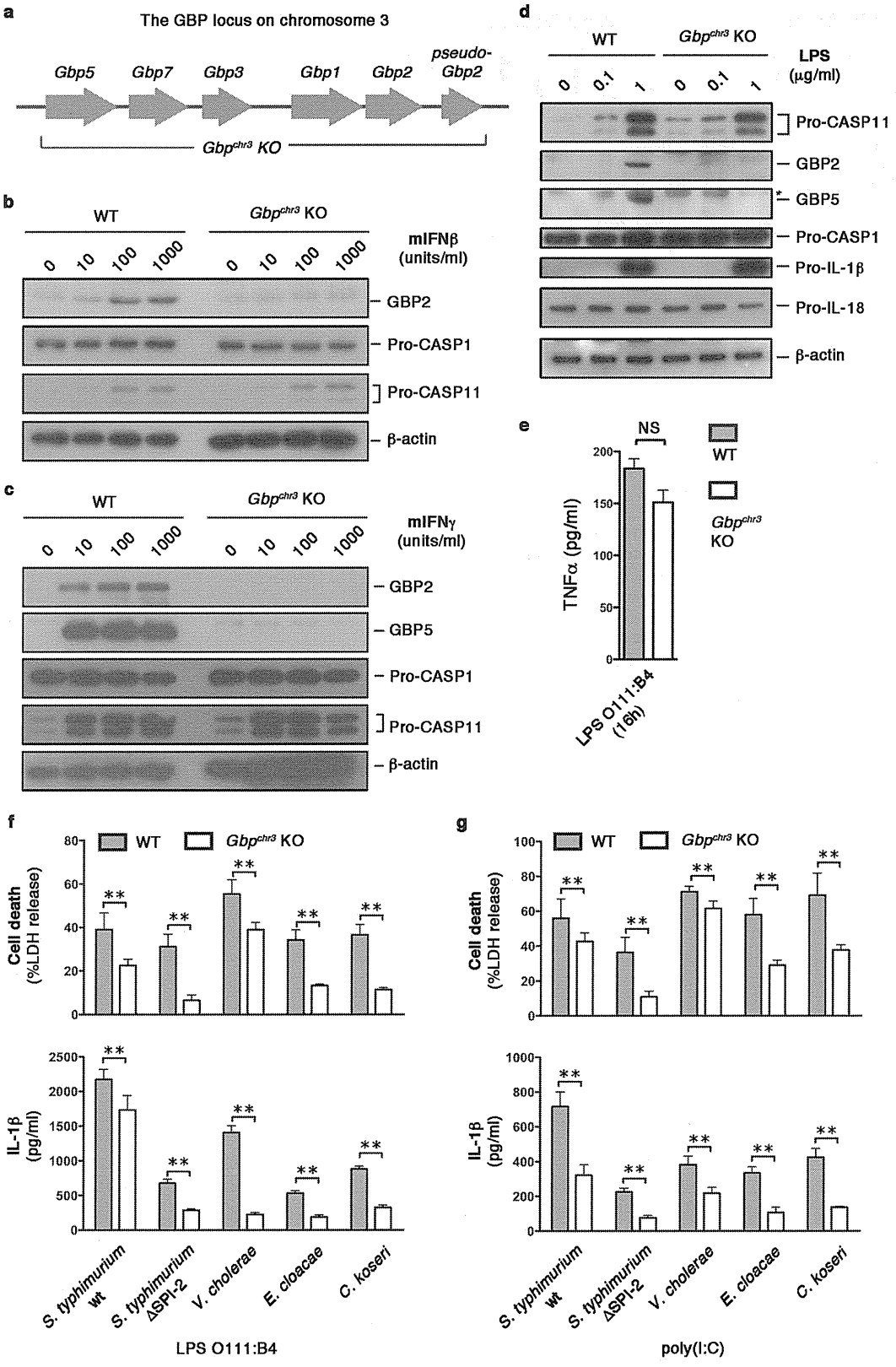

Extended Data Figure 2 | BMDMs from *Gbp*^{chr3} KO mice have normal responses to priming stimuli, but fail to activate the non-canonical inflammasome during bacterial infections. **a**, Schematic representation of the GBP locus on murine chromosome 3. The extent of the deletion in *Gbp*^{chr3} KO mice is indicated. **b–d**, Induction of pro-caspase-11, GBP2 and GBP5 expression in lysates of wild-type and *Gbp*^{chr3} KO BMDMs stimulated for 16 h with the indicated amounts of murine IFN-β, murine IFN-γ or LPS O111:B4. **e**, TNF-α release from BMDMs stimulated for 16 h with LPS O111:B4. **f**, **g**, LDH release and IL-1β secretion from wild-type and *Gbp*^{chr3} KO BMDMs infected for 16 h with wild-type (WT) *S. typhimurium*, ΔSPI-2 *S. typhimurium*, *V. cholerae*, *E. cloacae* or *C. koseri* grown to stationary phase. Cells were primed overnight with LPS (**f**) or poly(I:C) (**g**). *Indicates background band. Graphs show the mean and s.d. of quadruplicate wells and data are representative of two independent experiments. $^{**}P < 0.01$, NS, not significant (two-tailed *t*-test).

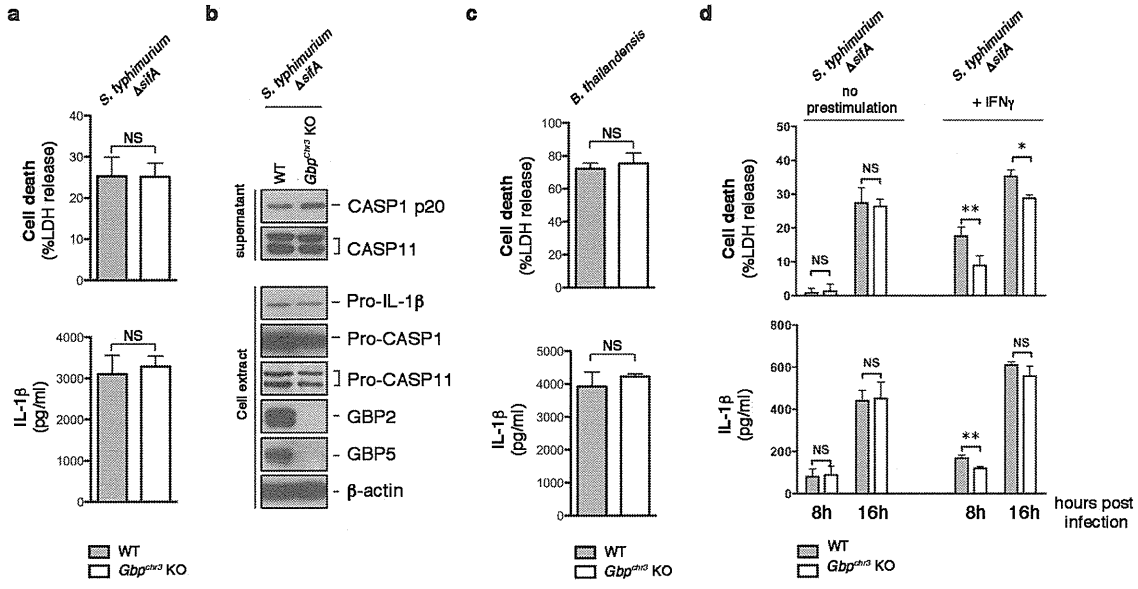

Extended Data Figure 3 | GBPs assist the detection of bacteria that escape into the cytosol only in primed macrophages. **a**–**c**, LDH release, IL-1β secretion and immunoblots for processed caspase-1 and caspase-11 released from unprimed BMDMs infected for 8–16 h with *ΔsifA S. typhimurium* or *B. thailandensis* grown to stationary phase. **d**, LDH release and IL-1β secretion from unprimed or IFN-γ-primed BMDMs infected for 16 h with *ΔsifA S. typhimurium* grown to stationary phase. Ext, extract; SN, supernatant. Graphs show the mean and s.d. of quadruplicate wells and data are representative of two independent experiments. $*P < 0.05$; $**P < 0.01$; NS, not significant (two-tailed *t*-test).

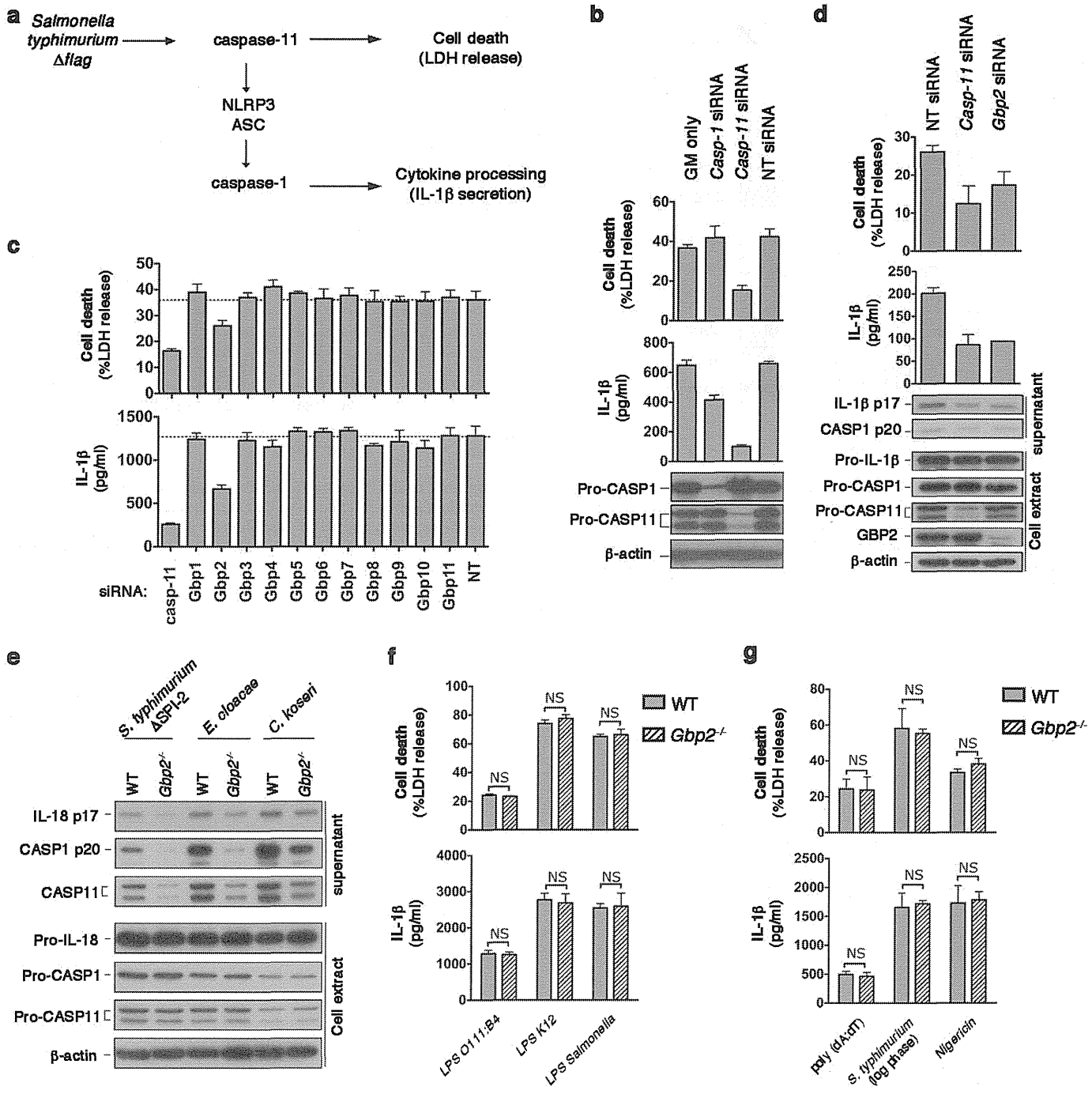

Extended Data Figure 4 | Murine GBP2 controls non-canonical inflammasome activation during *Salmonella* infection, but is dispensable for direct LPS sensing and canonical inflammasomes. **a**, Schematic drawing of the inflammasome pathways activated by flagellin-deficient *Salmonella*. **b–d**, LDH release, IL-1β secretion and immunoblots for processed caspase-1 and processed IL-1β released from unprimed BMDMs infected for 17 h with Δflag *S. typhimurium* grown to stationary phase. BMDMs were treated with the indicated siRNA for 56 h before infection. **e**, Immunoblots for processed caspase-1, IL-18 and caspase-11 released from unprimed BMDMs infected for 16 h with ΔSPI-2 *S. typhimurium*, *E. cloacae* or *C. koseri* grown to stationary phase. **f, g**, LDH release and IL-1β secretion from primed wild-type and *Gbp2*$^{-/-}$ BMDMs transfected with the indicated types of LPS for 16 h, treated with nigericin for 1 h, infected with SPI-1 T3SS expressing logarithmic phase wild-type *S. typhimurium* for 1 h, or transfected with poly(dA:dT) for 6 h. Cell were primed with PAM3CSK4 in **f** or LPS **g**. Graphs show the mean and s.d. of quadruplicate wells and data are representative of two (**e**) and three (**b–d, f, g**) independent experiments. NT, non-targeting siRNA; GM, GenMute transfection reagent; NS, not significant (two-tailed *t*-test).

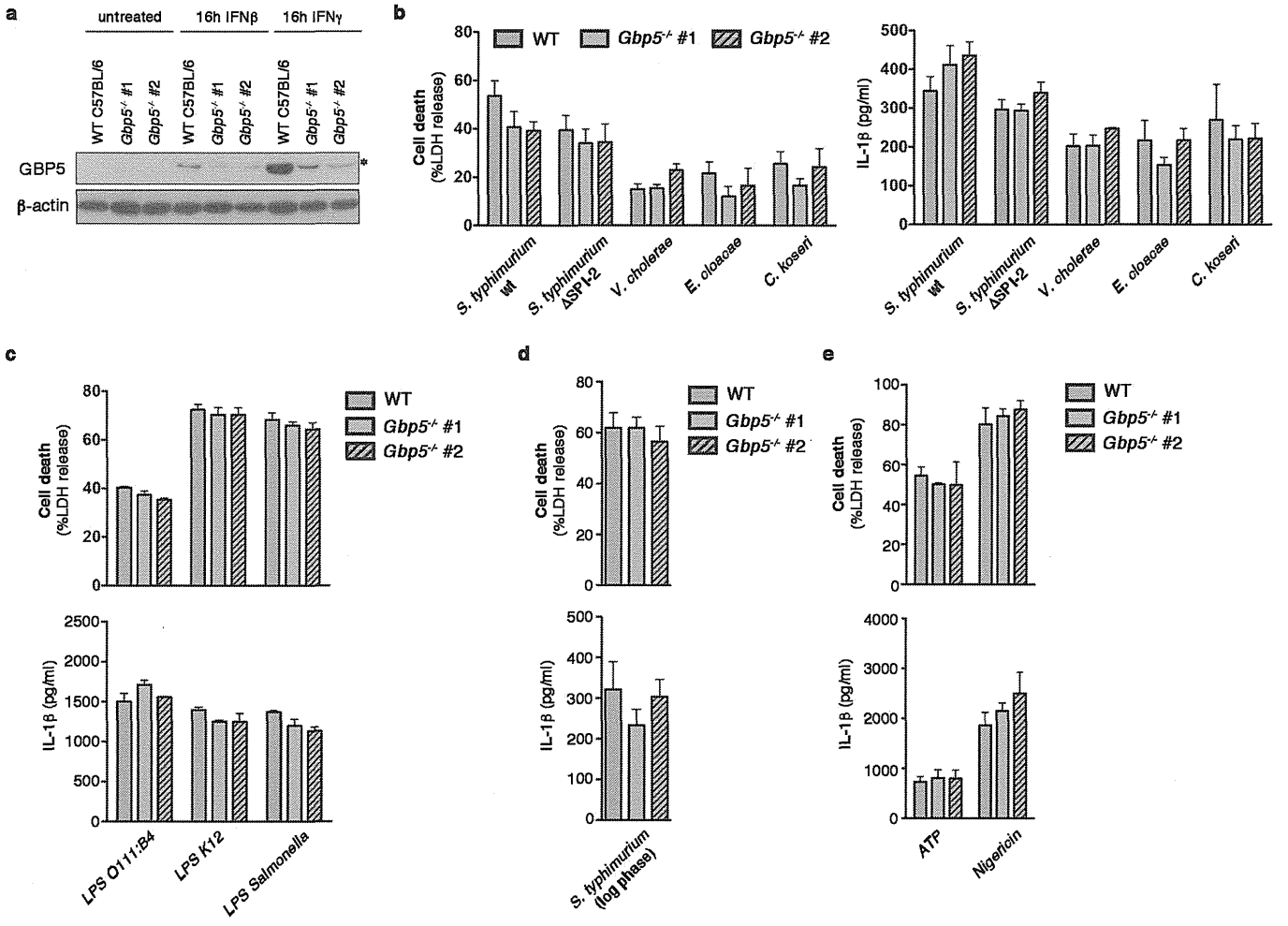

Extended Data Figure 5 | Normal activation of non-canonical and canonical inflammasomes in *Gbp5*$^{-/-}$ BMDMs. **a**, Expression of GBP5 in wild-type and two lines of *Gbp5*$^{-/-}$ BMDMs (1 and 2). *Indicates a cross-reactive band. **b–e**, LDH release and IL-1β secretion from BMDMs infected for 16 h with wild-type (WT) *S. typhimurium*, ΔSPI-2 *S. typhimurium*, *V. cholerae*, *E. cloacae* or *C. koseri* grown to stationary phase (**b**), transfected with the indicated LPS for 16 h (**c**) infected for 1 h with SPI-1 T3SS expressing logarithmic phase wild-type *S. typhimurium* (**d**), or treated with 5 mM ATP or 20 mM nigericin for 4 h (**e**). Cells were left unprimed (**b**) or primed with PAM3CSK4 in (**c**) or LPS (**d**, **e**). Graphs show the mean and s.d. of triplicate or quadruplicate wells and data are representative of three independent experiments.

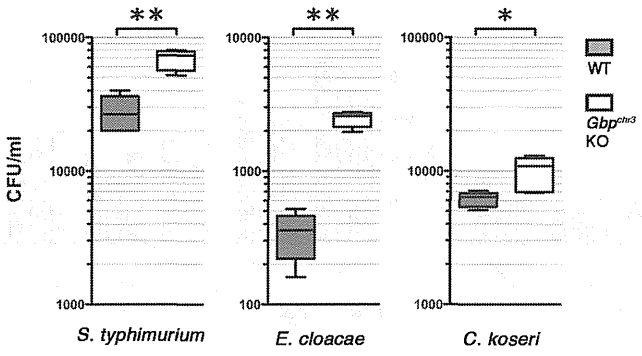

Extended Data Figure 6 | GBPs control bacterial replication. c.f.u.s at 16 h post-infection in wild-type and *Gbp*^{chr3} KO BMDMs infected with the indicated bacterial strains. Experiments are representative of two independent experiments.

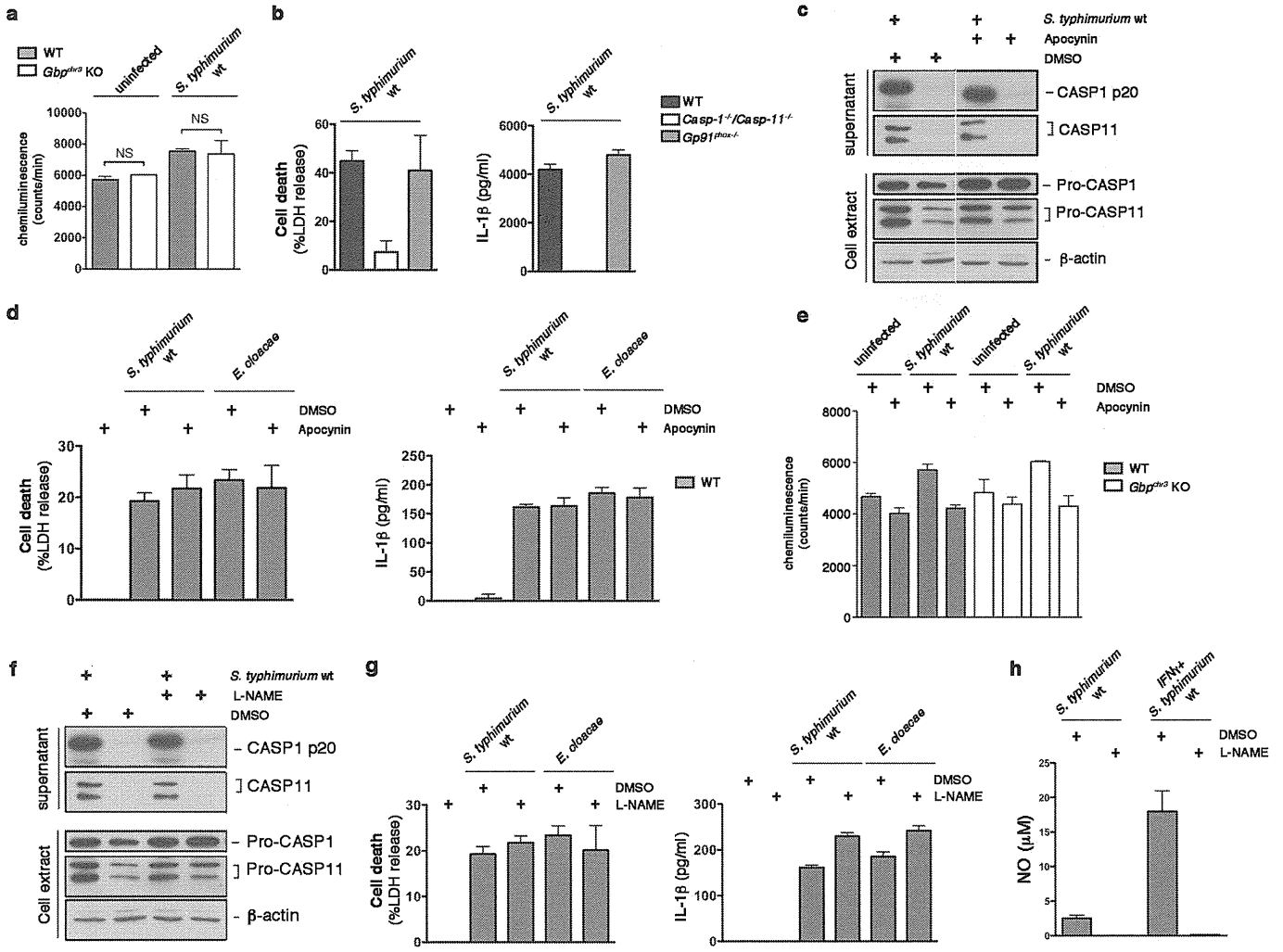

Extended Data Figure 7 | Inhibition of ROS and NO production does not affect non-canonical inflammasome activation. **a**, **b**, ROS levels, LDH release and IL-1β secretion in unprimed BMDMs left uninfected or infected for 16 h with wild-type *S. typhimurium* grown to stationary phase. **c**–**e**, LDH release, IL-1β secretion, ROS levels and immunoblots for processed caspase-1 and caspase-11 released from unprimed BMDMs infected for 16 h with wild-type (WT) *S. typhimurium* or *E. cloacae* grown to stationary phase in the presence of the ROS inhibitor (apocynin) or a vehicle control (DMSO). **f**, **g**, LDH release, IL-1β secretion and immunoblots for processed caspase-1 and caspase-11 released from unprimed BMDMs infected for 16 h with wild-type *S. typhimurium* or *E. cloacae* grown to stationary phase in the presence of the iNOS inhibitor (L-NAME) or a vehicle control (DMSO). **h**, NO release from unprimed or IFN-γ-primed BMDMs infected for 16 h with *S. typhimurium* in presence of the iNOS inhibitor (L-NAME) or a vehicle control (DMSO). Ext, extract; SN, supernatant. Graphs show the mean and s.d. of quadruplicate wells and data are representative of two (**a**–**c**, **e**–**g**) and three (**d**, **h**) independent experiments. NS, not significant (two-tailed *t*-test).

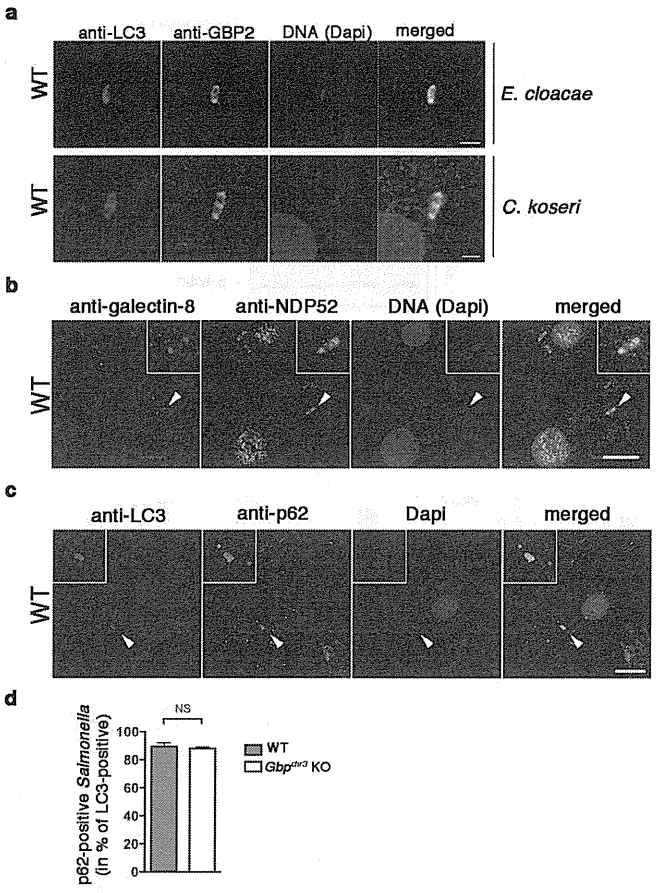

Extended Data Figure 8 | Colocalization of GBPs and autophagy proteins on intracellular bacteria. **a**, Colocalization of LC3 with GBPs in unprimed wild-type BMDMs infected with *E. cloacae* or *C. koseri* for 4 h and stained for LC3, GBP2 and DNA. **b**, Colocalization of galectin-8 and NDP52 in unprimed wild-type BMDMs infected with wild-type *S. typhimurium* for 4 h and stained for galectin-8, NDP52 and DNA. **c**, Colocalization of p62 and LC3 in unprimed wild-type BMDMs infected with wild-type *S. typhimurium* for 4 h and stained for LC3, p62 and DNA. **d**, Quantification of p62 and LC3 co-staining in wild-type and Gbp^{chr3} KO BMDMs at 4 h post-infection with *Salmonella*. Arrowheads indicate region shown in insets. Scale bars, 1 μm (**a**) and 10 μm (**b**, **c**). Graph shows the mean and s.d. of triplicate counts and images and graph are representative of at least two independent experiments. NS, not significant (two-tailed *t*-test).

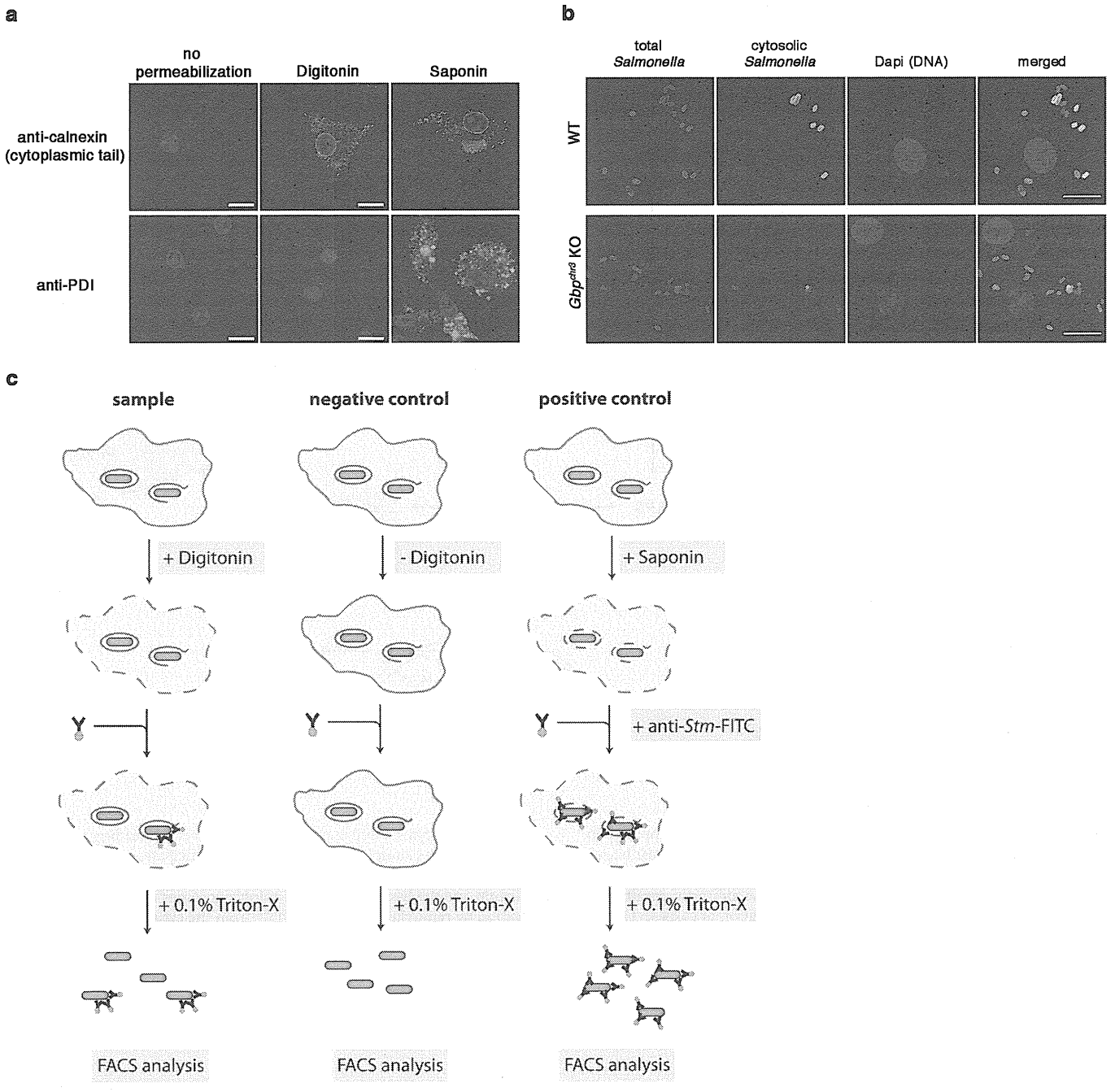

Extended Data Figure 9 | Digitonin-based quantification of cytoplasmic bacteria. a, Immunostaining for calnexin and PDI (protein disulphide isomerase) in wild-type BMDMs left untreated or permeabilized with digitonin or saponin. **b**, Differentially permeabilized macrophages stained for cytosolic and vacuolar *Salmonella* at 4 h post-infection. **c**, Schematic representation of FACS-based analysis of cytosolic and vacuolar bacterial populations of *Salmonella*. Scale bars, 10 μm.